4-2015

Supercontinuum Produced by Ultrashort Pulses from Ti:sapphire Laser and Nonlinear Photonic Crystal Fiber

Nicholas E. Maher

College of Saint Benedict/Saint John's University

Supercontinuum Produced by Ultrashort Pulses from Ti:sapphire Laser and Nonlinear Photonic Crystal Fiber

AN HONORS THESIS

College of St. Benedict/ St. John's University

In Partial Fulfillment

of the Requirements for Distinction

in the Department of Physics

by

Nicholas Maher

Advisor: Dr. Dean Langley

April 2015

Supercontinuum Produced by Ultrashort Pulses from Ti:sapphire Laser and Nonlinear Photonic Crystal Fiber

Approved by:

Dr. Todd Johnson
Assistant Professor of Physics

Dr. Adam Whitten
Adjunct Associate Professor of Physics

Dr. Dean Langley
Chair, Department of Physics

Dr. Emily Esch
Director, Honors Thesis Program

Abstract:

Producing a supercontinuum broadens the spectrum of the laser beam to potentially include the complete visible spectrum as well as some infrared and ultraviolet, providing a

more complete spectrum of selectable wavelengths. The supercontinuum is produced by nonlinear optical processes that occur when high intensity, ultrashort laser pulses are passed through a photonic crystal fiber. In this project, a mode-locked Ti:sapphire laser was manually constructed to observe the supercontinuum effect.

Introduction:

In the past few decades, lasers have been applied to various fields including medicine, manufacturing, spectroscopy, and telecommunications. Some applications require laser beams at a specific wavelength, but lasers are typically limited to a single wavelength or a small spectral bandwidth (1-100 nm) that is determined by its gain medium, making it difficult to be selective of wavelength. However, a supercontinuum can use a mode-locked laser of any wavelength to create new wavelengths within the laser beam and broaden the spectrum.

The supercontinuum is produced by nonlinear optical processes that occur when high intensity, ultrashort laser pulses are passed through a photonic crystal fiber (PCF). Physicists are still trying to understand all of the nonlinear processes that are responsible for this effect, but self-phase modulation (SPM) has been indicated as an underlying contributor. In this project, a mode-locked Ti:sapphire laser was manually constructed with a wavelength spectrum of 800-820 nm and applied to a PCF with a zero-dispersion wavelength (ZDW) of 800 nm. A Frequency-Resolved Optical Gating (FROG) was used to analyze the laser beam before and after the supercontinuum process to demonstrate the SPM that occurs within the PCF. Although the resultant supercontinuum beam was too weak to be detected by the FROG, the spectrum broadened to 750-860 nm. The possible

factors responsible for this loss of power and short broadening are considered for future research.

Each aspect of the research will be broken into sections and discussed in further detail. First, I will briefly explain how lasers function. Then, we will move on to how the Ti:sapphire laser was constructed and the significance of each of its pieces. Following, I will cover how the laser was set in the mode-locked state. Next, I will explain the design of the PCF and how it was implemented, and then the design of the FROG and its significance in this project. Finally, I will cover the results of our attempt at producing a supercontinuum and what room this leaves for future research.

In order to fully understand the method used to achieve the goals set in this project, a small background of lasers is necessary. A laser (Light Amplification by Stimulated Emission of Radiation) is produced by exciting atoms coherently through stimulated emission. When an atom receives enough energy by absorbing energy from the incident photon, its electrons will jump to an excited or higher energy state. Then, the atom will release the energy by emitting a photon and returning to its natural, stable state. This photon stimulates other atoms to produce photons in the same direction, as seen in Figure 1.

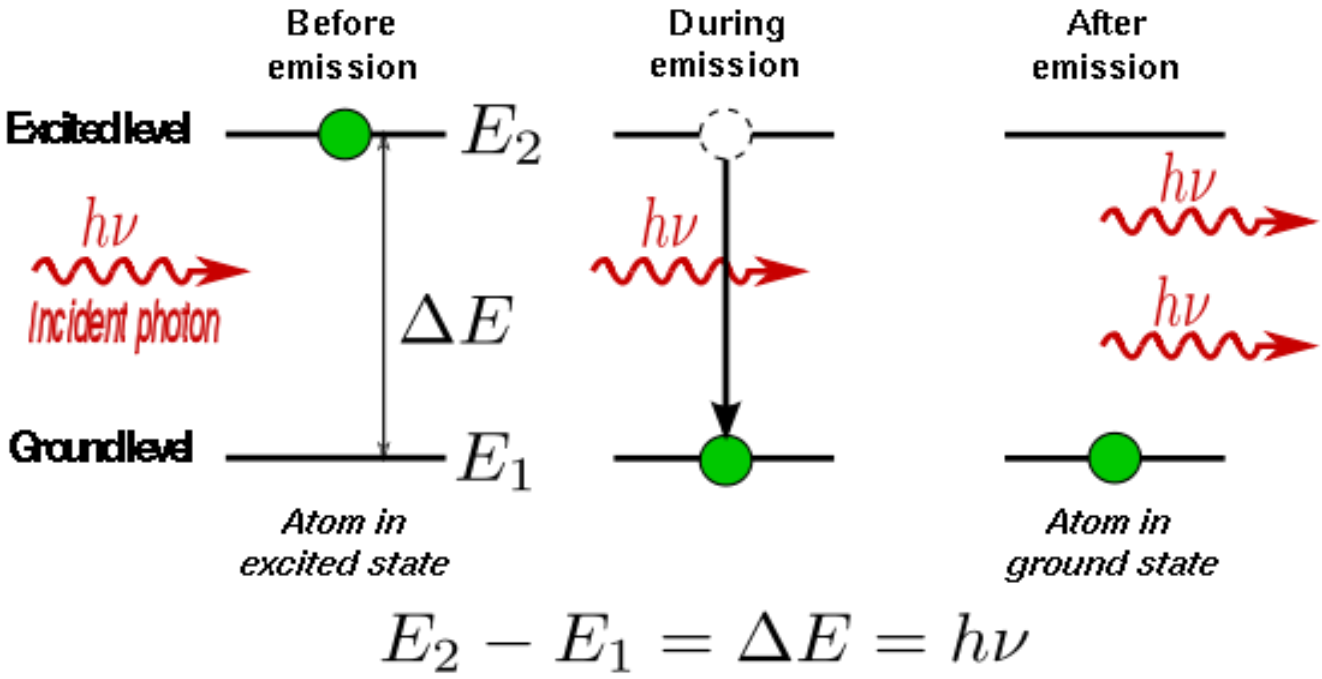

Figure1: Stimulated emission occurs when an incident photon excites an atom to release another photon in the same direction. The lower equation expresses how the change in energy creates a photon of frequency *v* and Planck's constant *h*. Image Source: http://en.wikipedia.org/wiki/Laser#/media/File:Stimulated_Emission.svg.

By using two mirrors, the photons are passed back and forth through the gain material (in this case the Ti:sapphire crystal) in what is called the laser cavity, amplifying the light, as seen in Figure 2. The high reflector is almost perfectly reflective (99.9% reflected) and reflects almost all light back through the medium. The output coupler is 92-98% reflected, so once enough photons have been produced, some will pass through the mirror and create a continuous beam.

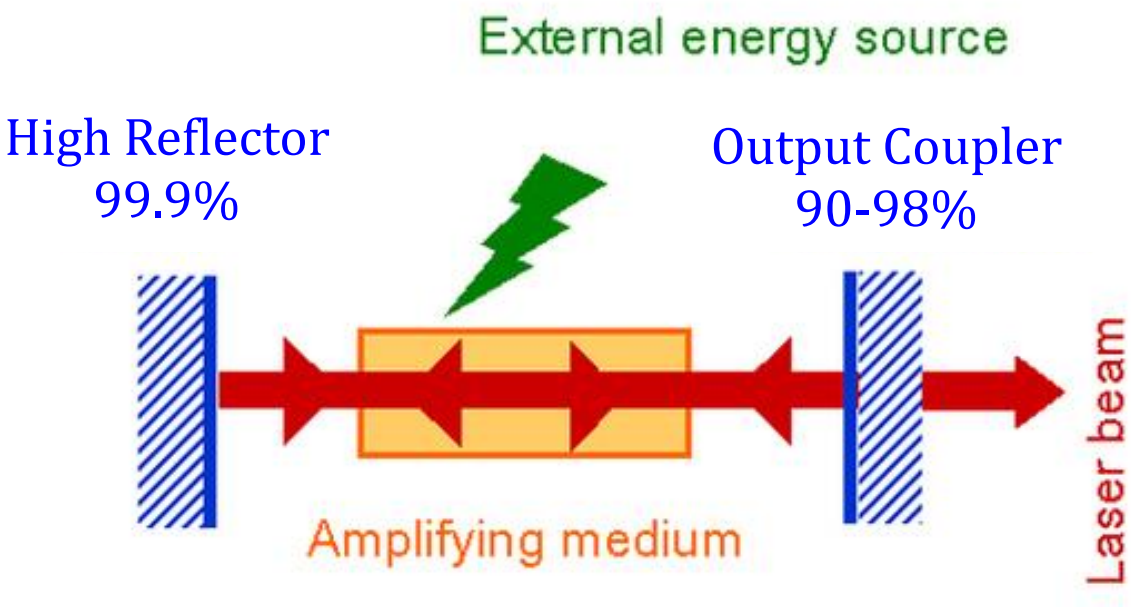

Figure 2: The external energy source (Verdi laser) passes through the amplifying medium (Ti:sapphire crystal). The high reflector and output coupler reflect the light back and forth through the amplifying medium until a laser beam is produced that refracts through the output coupler. Image Source: http://www.optique-ingenieur.org/en/courses/OPI_ang_M01_C01/res/fig01.jpg.

The light waves within the laser cavity will reflect between the mirrors, forming standing waves called modes. When the modes interfere with each other, they create a random beating, which averages to a continuous wave. This is due to constructive and destructive interference of the waves. When the modes move in phase with one another, they will periodically constructively interfere and destructively interfere, creating pulses at a consistent rate, otherwise known as mode-locking.

Laser Construction:

For this experiment, a mode-locked Ti:sapphire laser was used to achieve the supercontinuum process. Optics distributors such as ThorLabs sell supercontinuum generation kits for $14,630 (ThorLabs.com). To avoid this price, a PCF was bought for

$1,555.00 to produce the supercontinuum manually and more cost-efficiently. This involved constructing a Ti:sapphire laser and aligning it with the PCF by hand. A mode-locked laser is needed to produce the ultrashort pulses necessary to allow for nonlinear occurrences in the photonic crystal fiber (PCF). A Titanium doped sapphire (Ti:sapphire) crystal is a good gain medium to produce a pulsing laser. The compound of sapphire doped with Titanium is atomically designed to absorb a green beam and can fluoresce at anywhere between 680 nm and 1050 nm (red to infrared region). In our case, the crystal was pumpeded with 5.00 W of a Coherent Verdi 532 nm laser beam and produced an 810±10 nm output beam. Henceforth, pump power will refer to the power of the Verdi laser as it is pumping the Ti:sapphire laser. A layout of the laser can be seen in Figure 3.

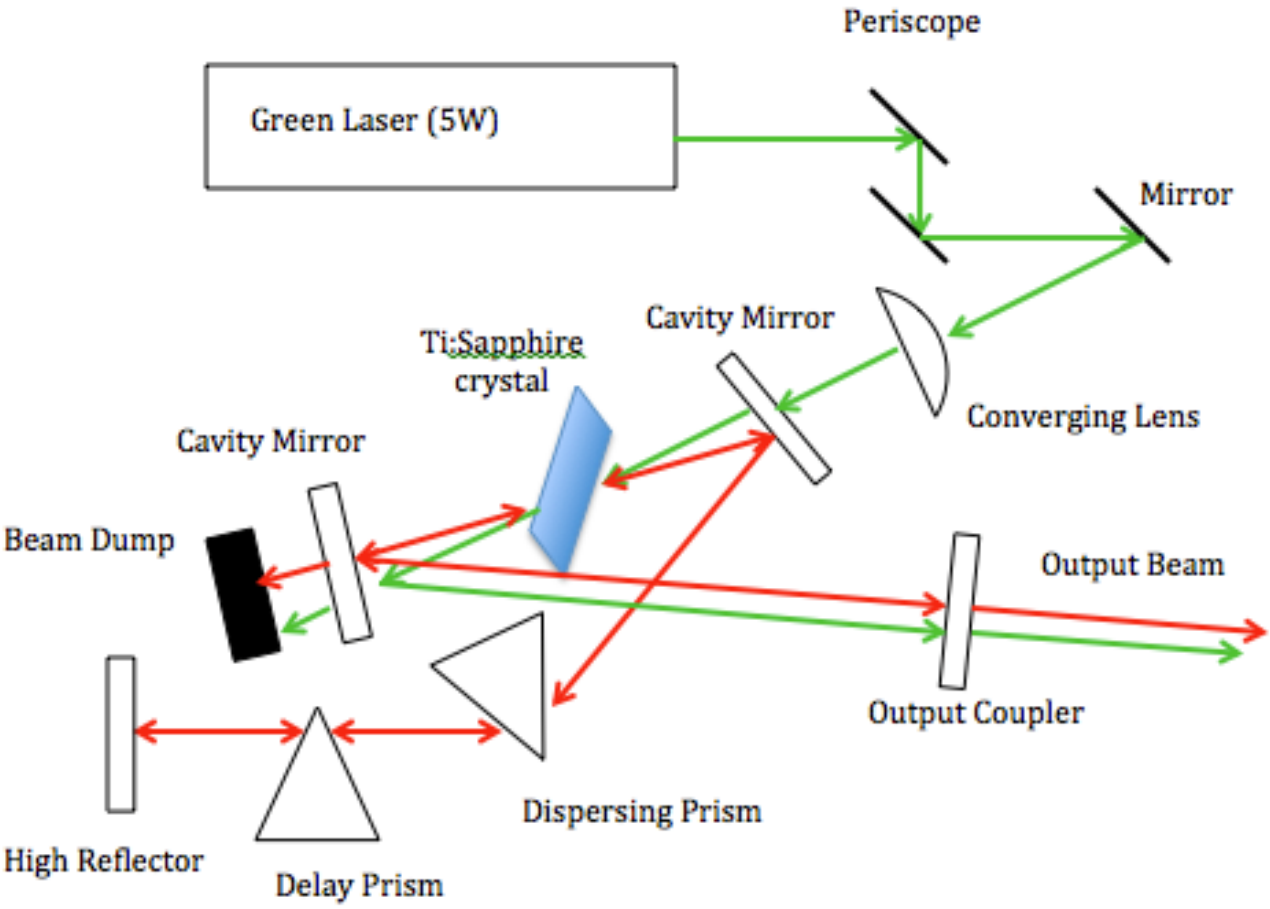

Figure 3: The layout of the Ti:sapphire laser that was constructed to send ultrafast pulses at about 800nm. The green arrows represent the Verdi pump laser beam and the red arrows represent the Ti:sapphire laser beam.

The entire laser was constructed on a table whose legs were suspended by pressurized air to ensure that the table was level and stable. Both the Verdi laser and the sapphire crystal had separate temperature controllers that cycled water to keep them from overheating and causing harm. The crystal cooler was set at 30.00°C and the Verdi cooler was set at 21.74°C. The distances and angles between the mirrors, crystal, and prisms were based off of calculations made by the Washington State University Physics Department, who published a document explaining how to construct a mode-locked Ti:sapphire laser (Kapteyn 1992). Their design aims to produce a stable self-mode-locking laser with pulse

widths shorter than 11 femtoseconds (Kapteyn 1992). In the construction of the laser, we referenced steps suggested by Washington State University and Kapteyn-Murnane Laboratories (Kapteyn 1992, Kapteyn-Murnane 2000). Although the Ti:sapphire laser at St. John's University had been constructed from past undergraduate research based off of these documents, the whole system was reconstructed from scratch to ensure that the mirrors were aligned precisely. However, the output coupler, high reflector, and prisms were left in their original fixed positions as specified by Figure 4.

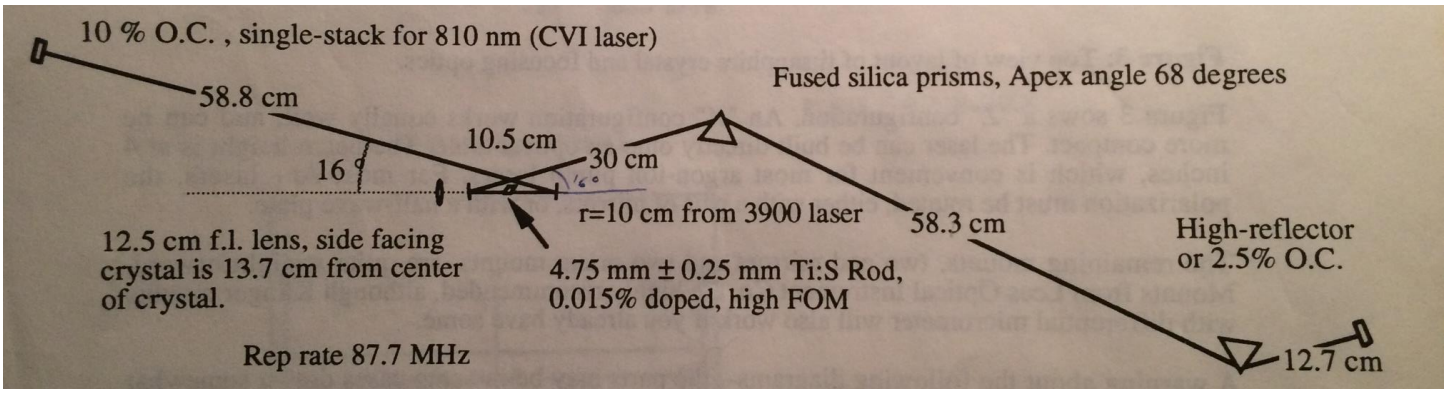

Figure 4: Washington State University's distances and angles for the setup of a mode-locked Ti:sapphire laser. The arrow points to the location of the crystal, with two cavity mirrors on either side. The triangles represent the delay prism and dispersion prism. The high reflector of 99.9% reflection is on the far right while the output coupler (OC) of 90% reflection is on the far left. Image Source: Kapteyn 1992.

In order to allow the lasing to occur, the green laser beam had to be polarized parallel to the table. This allows the photons to behave coherently and emit in phase. The Verdi laser beam was naturally polarized perpendicular to the surface it sat on, but we had to ensure that the laser beam polarization remained parallel to the table while it propagated towards the Ti:sapphire crystal. Using a periscope consisting of two slanted mirrors as shown in Figure 5, we were able to lower the height of the beam and rotate the polarization of the beam 90° to a horizontal orientation, parallel with the table.

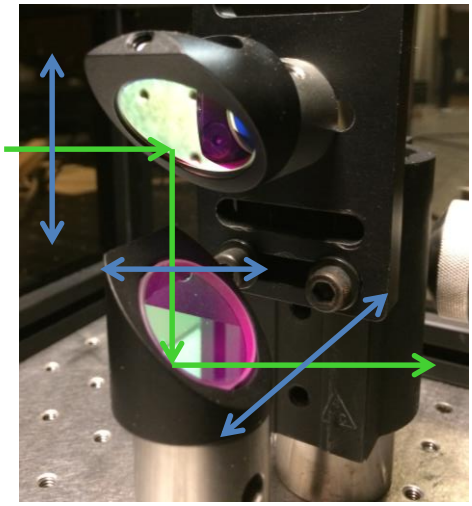

Figure 5: This is the periscope used to set the beam at the desired height of 87.5mm. The green arrows represent the path of the Verdi laser beam and the blue arrows represent the polarization of the laser beam. The first mirror is set at an angle that orients the beam vertically downward so that it can reach the desired height. A receiving mirror is positioned to reflect the beam at 87.5mm, the same height as the crystal, and angled to reorient the beam parallel to the table.

The Verdi laser was set to a pump power of 0.01W during the alignment process for safety. Throughout the setup, to ensure that the laser beam was oriented parallel to the table at 87.5mm, the beam was measured to this height at a distance as far away from the mirror as the table would permit. If the height of the beam remains at a constant height over a long distance, it can be considered parallel to the table.

The beam then passed through a converging lens that was focused on the center of the crystal, as seen in Figure 6. The crystal and two cavity mirrors were set on a rail so that the distances between the mirrors and crystal could be easily altered. The 12.5 cm focal length lens was inserted so that the beam enters through the curved edge first. To align the lens, the lens mount was manipulated so that the beam was set at the constant height to the edge of the table and aimed down the center of the rail. The resulting beam then hit a spot on the wall that was marked for easy reference.

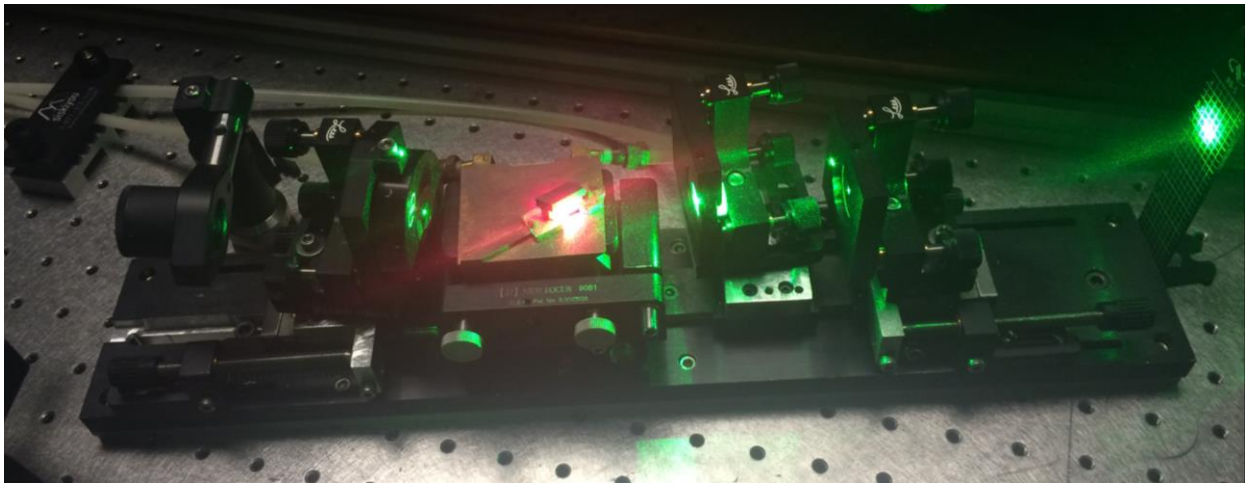

Figure 6: This figure shows the track that was used to position each mirror. From left to right positioned on the rail is the beam dump, the second cavity mirror, the Ti:sapphire crystal on the copper stage, the first cavity mirror, and the focusing lens.

The converging lens causes the Kerr-effect, which allows for self-mode-locking. Focusing the laser beam into the center of the crystal significantly increases the intensity of the pump laser beam within the crystal. A laser beam is an electromagnetic wave and when it is passed through a dielectric medium, the material is polarized by the alternating electric field of the beam. The relation between polarization and the electric field is represented by Equation 1 (Pedrotti 1993).

$$P = \epsilon_0(\chi_1 E + \chi_2 E^2 + \chi_3 E^3 + \cdots) \quad (1)$$

Here, P is the polarization, ϵ_0 is the electric permittivity of free space, χ is the susceptibility, and E is the electric field. The first term in the power series represents linear media and the higher order terms represent nonlinear media. In linear optics the electron oscillations are small and the polarization is proportional to the electric field. However, the electric field increases with an increase in intensity. Consequently, for high intensities the

nonlinear terms become significant because the electrons cannot oscillate at the same frequency as the changing electric field, causing nonlinear polarization (Pedrotti 1993).

Similarly, for low intensities, the index of refraction of a medium remains constant. However, for Kerr media such as Ti:sapphire crystals, when high intensity light passes through the crystal gain medium, the index of refraction begins to depend on the intensity. This is known as the Kerr-effect, which is a third-order nonlinear process as shown in Equation 2 (Pe'er 2013).

$$n = n_0 + n_2 I \tag{2}$$

Here, n_0 is the linear index of refraction, n_2 is the nonlinear index of refraction, and I is the intensity of the beam. Since a larger index of refraction means a larger angle of refraction through the medium, the beam is focused, effectively shrinking the beam waist. This process is known as self-focusing. The beam is not infinitely focused to a point source because eventually the dispersion effect of the Gaussian beam counteracts the Kerr effect. This can be seen in Figure 7.

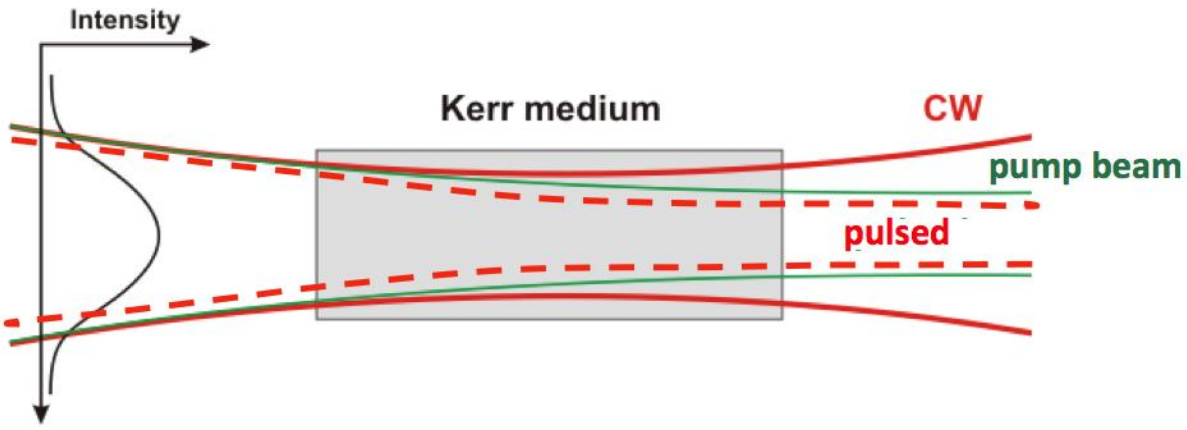

Figure 7: This figure represents the Kerr effect on the pump beam (green) and the produced laser beam (red) within the Ti:sapphire crystal (CW and pulsed). Initially, both beams propagate from the left. The Kerr effect then focuses the high intensity light. If the Ti:sapphire laser has a continuous wave beam (solid red), the beam does not self-focus enough to fit within the pump beam "aperture." This then crops off the low intensity edges of the beam, and results in a high intensity beam that is mode-lock preferable. Since a pulsed beam (dashed red) consists of high intensity pulses, it self-focuses enough to fit inside the pump beam. Image Source: http://upload.wikimedia.org/wikipedia/en/0/07 /Kerr-lens_Modelocking.png.

The Kerr effect acts as a saturable absorber, which makes the mode-locked state more preferable than the continuous wave state. A saturable absorber absorbs lower-intensity light and allows higher intensity light to pass with less absorption (Miller 2011). Within the crystal, the pump beam and the ~800nm laser beam being produced by the amplification of the crystal gain medium are overlapping. The pump laser, which is set at 5.00 W output, is sufficiently intense to self-focus due to the Kerr effect. This pump laser beam acts as an aperture within the crystal medium so that only the high intensity ~800nm light that has also undergone the Kerr effect passes with minimal absorption, while low intensity light experiences higher loss. Thus, high intensity peak pulses pass more easily than a continuous, lower intensity wave. Essentially, the saturable absorber crops the low intensity edges of the beam and passes the high intensity center of the beam. This makes

high intensity pulses preferable because the pulses do not get clipped by the saturable absorber. Because the Kerr effect occurs almost instantaneously, it can create the ultrashort pulses (Pe'er 2013).

Next, the first cavity mirror, which has a focal length of 10 cm, was inserted on the track. The cavity mirror closest to the output coupler in Figure 4 will be referenced as the first cavity mirror. The mirror mount was translated and elevated to ensure that the beam hit the center of this mirror and the mark on the wall. To achieve the 16° angle reflection of the laser beam from the first cavity mirror to the first prism according to the position determined in Figure 4, the mirror was rotated 8° towards the prism. Also, the mirror was slid forward and backward on the rail to make sure that the beam still hit the mark on the wall. However, the lens should be left about 10 cm away from the crystal location so that the beam is focused within the crystal.

A special stage was constructed to hold the crystal for alignment purposes. The crystal itself is in a rhombus prism shape and was encased in a copper holder set on a copper stage. The copper holder covers the top and sides of the crystal, leaving two opposite faces open for the beam to pass through. The copper allows for the water coolant system to keep the crystal cool without making physical contact with the crystal. The copper stage was set on a stage that can be rotated horizontally, as well as translated parallel to the rail and perpendicular to the rail. The crystal was positioned so that the beam traveled through more or less its center. Then, the crystal was rotated and translated to find the Brewster angle. This is the angle at which there is minimum reflection of the beam. A power meter was used to measure the intensity of the reflection and the pump

laser was increased to 0.5W for more sensitivity of the power meter. The power meter uses a thermal head to measure the power of the laser beam.

The second cavity mirror, also with a focal length of 10 cm, was then aligned similar to the first cavity mirror, with the mirror tilted 8° so as to reflect the beam at 16° towards the output coupler as in Figure 4. A beam dump was inserted behind the second cavity mirror to contain any excess beams that refract through it. The prisms, high reflector, and output coupler were left unmoved from the previous setup, positioned at the distances specified in Figure 4.

A mode-locked laser requires that the pulse maintains a constant spatio-temporal shape. This means that the light waves are traveling in phase spatially and at the same speed through air. However, dispersion that occurs within the Ti:sapphire crystal stretches the beam so that the larger wavelengths are ahead of the lower wavelengths in space and time. Hence, two fused silica prisms were introduced between the high reflector and the gain medium to counteract the dispersion. The prism pair cooperates to ensure that the wavelengths travel the same distance within the cavity and the frequencies have a net group velocity of zero.

The laser beam hits the first prism near the tip, which then spreads the wavelengths out spatially, so that they hit the second prism at different thicknesses. The second prism is oriented so that the longer wavelengths have to travel through more of the prism, and the shorter wavelengths travel closer to the tip. The larger wavelengths will be slowed down by traveling through a greater thickness of the prism than the shorter wavelengths (Pe'er 2013). These prisms were set in platforms aligned by the manufacturer so that the beams are refracted parallel to the surface they sit on.

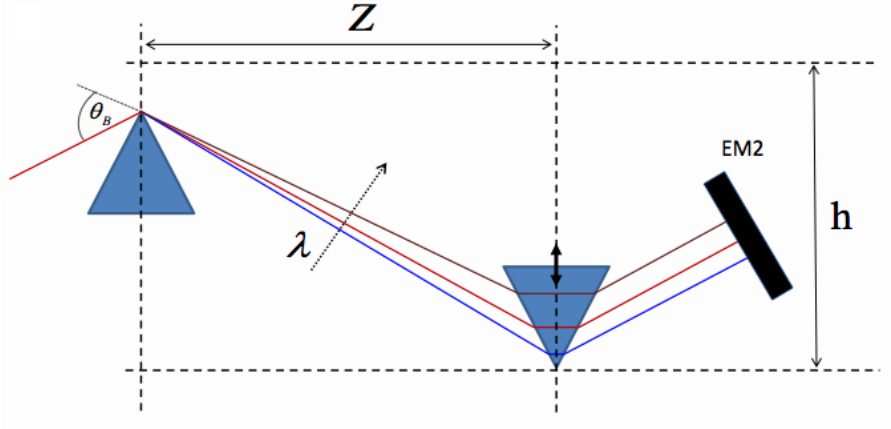

Figure 8: The prism pair uses the index of refraction of the prisms to spread out the wavelengths spatially and travel different distances and at different speeds to counteract dispersion. λ indicates that the wavelength increases from blue to red to infrared. EM2 represents the high reflector, which sends the laser beam back along the same path. Image Source: Pe'er 2013.

After setup, the Verdi laser pump power was increased to 5W to achieve lasing. This pump power was the most successful at producing the Ti:sapphire laser beam. A power meter was placed on the outside of the output coupler to check for lasing. Any light intense enough to be detected on the opposite side of the output coupler would be considered lasing. Adjustments were made particularly to the high reflector and output coupler, as well as the cavity mirrors until lasing occurred. The output power was then optimized using the power meter and adjusting all mirrors. Usually the output power was between 0.40 and 0.50 W, measured after the samples and in the mode-locked state with the Verdi laser set to pump at 5.00W. However, on good days, the laser reached a peak power of 0.80 W.

Mode-Locking:

For easier mode-locking, the green and red laser beam spots on the first cavity mirror were observed. Since the wavelengths of the Verdi laser beam and the Ti:sapphire laser beam are different, they are refracted by the crystal at different angles when they transfer from the crystal medium to air. Consequently, the green laser beam spot is slightly

to the left of the red laser beam spot. For best results, the high reflector and output coupler should be adjusted so that the center of the red spot is about a millimeter to the right of the green spot, while still overlapping. This ensures that the two beams are overlapping as much as possible within the crystal.

In order to detect whether the laser beam was in the mode-locked state, multiple detectors were positioned at the output of the laser, as displayed in Figure 9. The pulses occur too quickly for the eye to tell the difference between a mode-locked or continuous beam, so an oscilloscope, a beam map, and a spectrometer were used to determine which state the laser beam was in. Note that the beam first passes through a long-pass filter before being measured. The filter blocks any wavelengths shorter than 500nm and passes longer wavelengths. This ensures that the Verdi laser which has been propagating alongside the Ti:sapphire laser beam is blocked from detection. The pellicle redirects only a sample of the laser beam so that only 8% of the beam's power is removed from the system for detection and the rest is allowed to pass through and continue on to the PCF. A second pellicle is used to split this sample beam so that half is sent to the oscilloscope and the other half to a spectrometer.

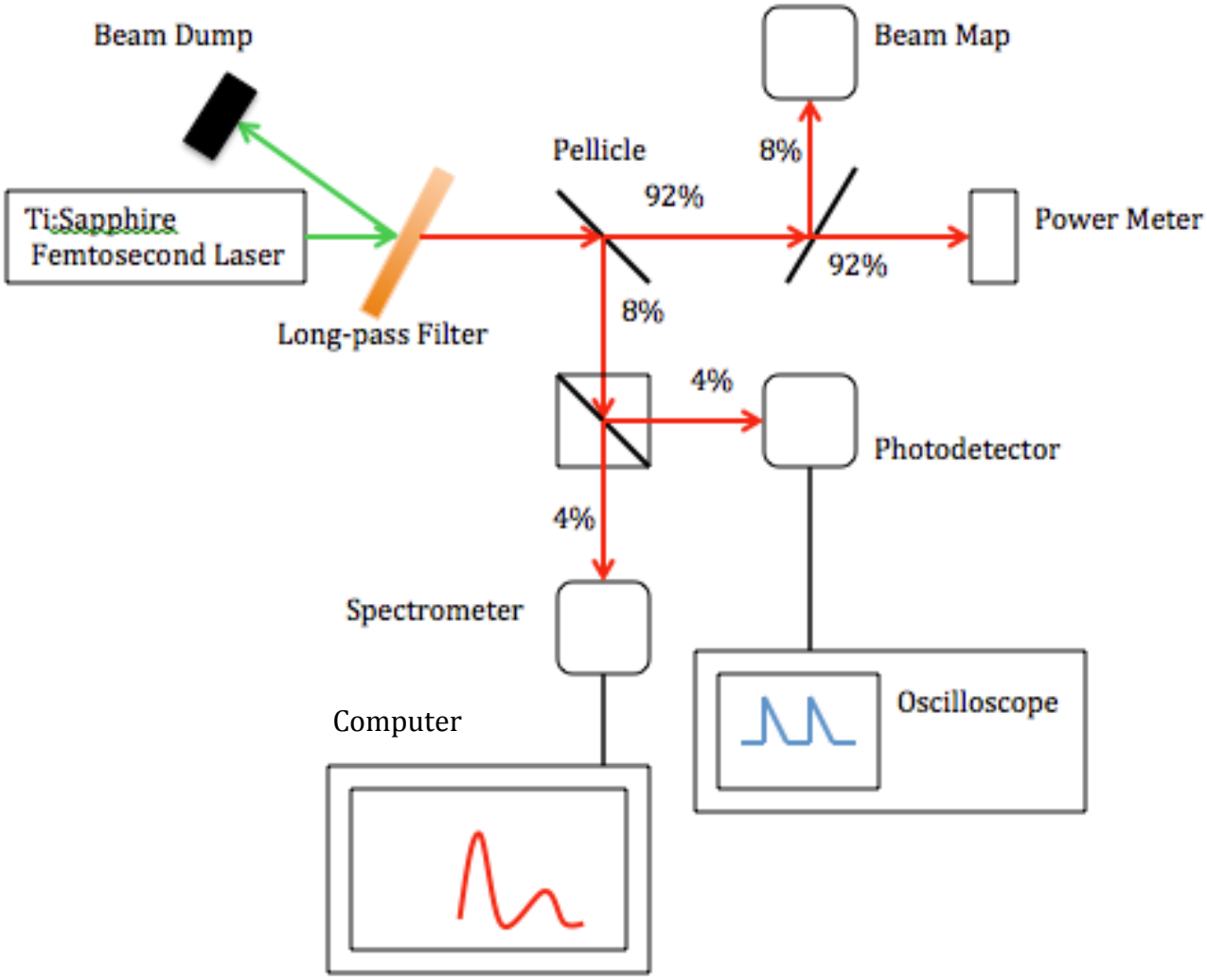

Figure 9: This diagram displays the devices used to analyze the pulses from the laser and their placement. Pellicles are used to direct the beams to the various detection devices.

An oscilloscope uses a photodetector to observe the intensity of the laser beam over time, indicating whether it is continuous or pulsing. A snapshot of a mode-locked laser pulse is shown in Figure 10. A continuous wave shows up as noise on the oscilloscope because the electromagnetic field is changing randomly. However, a mode-locked laser pulse would show up as peaks of electromagnetic intensity at consistent intervals. Once these peaks appear and remain stable, the laser is mode-locked.

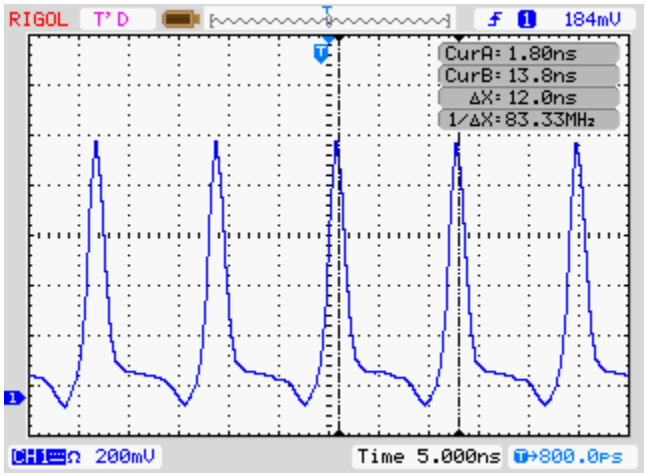

Figure 10: This snapshot of the oscilloscope illustrates the pulses from the laser. The pulse is too quick for the oscilloscope to capture accurately so it estimates, creating dips before the high intensity peak. Also, the peaks are actually thinner than the oscilloscope can depict, but are roughly sketched by the oscilloscope as wide peaks. Image taken from oscilloscope screen. 1/Δx on the upper right represents the frequency of the pulses.

These peaks are due to the constructive superposition of modes within the cavity that reach peak intensity. Due to limitations of the device, the pulses are too fast for the device to accurately depict. Rather than a sharp peak, it is depicted to have a rounded edge. The oscilloscope is also used to measure the frequency of the pulses, which as shown in Figure 10 was about 83MHz.

We use spectrometers to measure the wavelengths present in the beam for mode-lock detection. A continuous wave would have a column of intensity at the lasing wavelength (around 800 nm), while a mode-locked spectrum would be broader.This is because the wavelengths are moving in phase together within the pulses. This can be seen in Figure 11, where the mode-locked laser beam spectrum is about 25 nm wider.

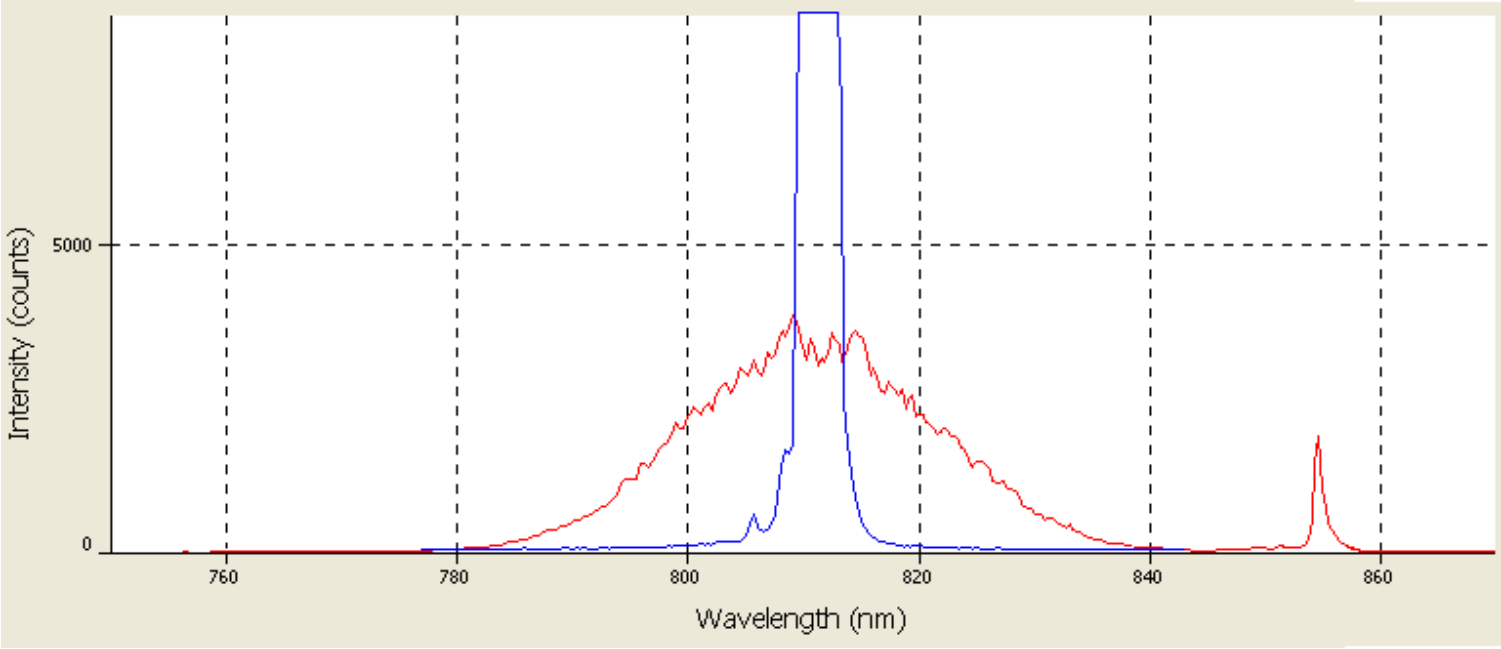

Figure 11: This figure is a screenshot of two spectrometers which measure the intensity of wavelengths present in the observed laser beam. The blue line represents the spectrum of a continuous wave laser beam and the blue line represents the spectrum of a mode-locked laser beam.

Besides the interval of the pulsing and the laser beam's wavelength spectrum, the shape of the pulse was also detected. A beam map CCD camera effectively observes the cross-section of the laser pulse and measures its size and shape, as well as the intensity of the beam throughout this area. An example of the beam map is shown in Figure 12. A mode-locked beam would be circular with an ellipticity of 1.00 and a Gaussian shaped intensity, known as a Transverse Electromagnetic Mode of 00 (TEM00). While mode-locking the laser, the beam should become more oval shaped.

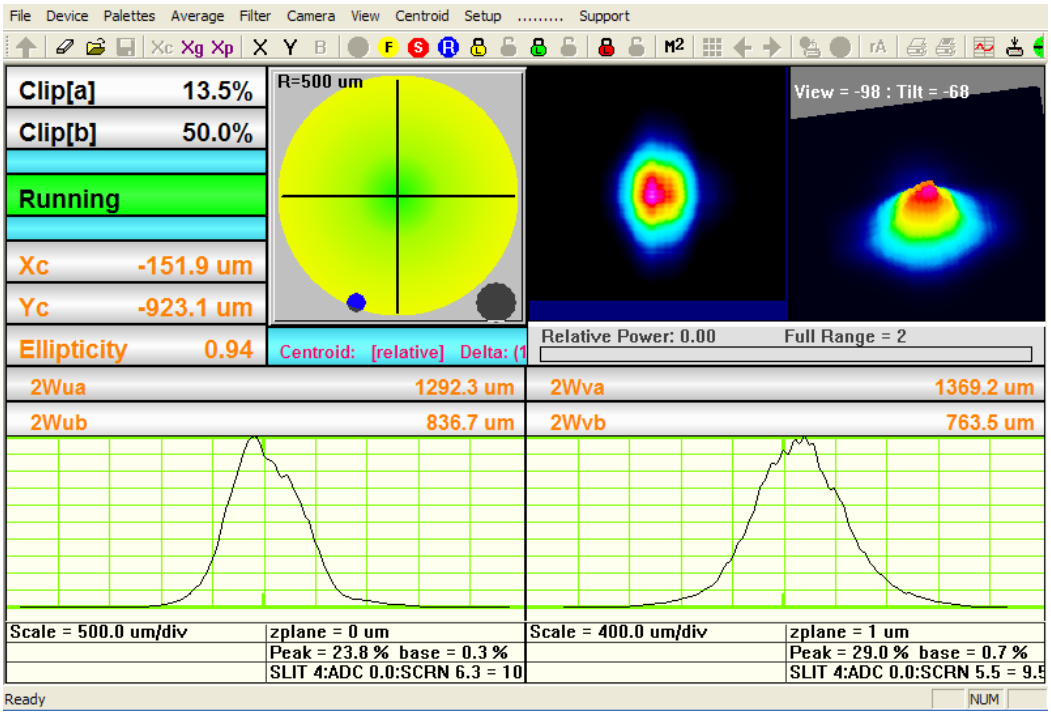

Figure 12: This is a beam map of the Ti:sapphire laser beam. The far right 3D model represents the intensity of the beam with red being the most intense. Adjacent is the 2D cross-section of the beam and below are vertical and horizontal "slices" of the 3D intensity model. The far left graph displays where the center of the beam is hitting with reference to the center of the sensor. The location is measured in μm by Xc and Yc to the left. The ellipticity measures how circular the beam is. Clip[a] and clip[b] are the percentages of the full height of the bottom curves at which the width is measured. Clip[a] represents $1/e^2$ and clip[b] represents the full width half maximum (FWHM), both widely accepted heights at which to measure the width of a Gaussian curve. The 2Wua represents the diameter of the beam at 13.5% of the maximum intensity and 2Wub is at FWHM.

Mode-locking requires some luck and some acquired skill, but there is a general process that is suggested by both Kapteyn-Murnane Labs and Washington State University (Kapteyn 1992, Kapteyn-Murnane 2002). The first step involves sliding the second cavity mirror along the rail and monitoring the beam map. According to Dr. Greg Taft, a St. John's University alumnus who has thoroughly researched Ti:sapphire lasers and works for Kapteyn-Murnane Laboratories, the second cavity mirror has two regions in which it lases well, with a small region between in which it will not lase. For mode-locking, the mirror should be in the region farthest from the crystal. Then, the other mirrors and crystal were

adjusted until the power was optimized and a TEM00 mode was observed on the beam map. The delay prism was then pulled out from the laser beam path (so that less of the tip was exposed to the beam) as much as possible without decreasing the power. The second cavity mirror was then slid towards the crystal until it reached the edge of the stability region, at which point the beam map showed a more horizontally elongated beam.

The final step is as simple as rocking the delay prism to cause self-mode-locking. The prism platform was designed with a spring so that it could be nudged horizontally with a finger. The nudge gives the wavelengths the spatial push to fall into phase with each other. Success would be indicated by stable peaks on the oscilloscope that last longer than a few minutes, a slightly wider spectrum on the spectrometer, and a beam map displaying a TEM00 mode beam again.

This process never worked on the first try. To troubleshoot, the second cavity mirror was slid at small increments and then the power was optimized. The delay prism was then inserted or removed slightly and nudged. When the laser was close to mode-locking, the pulses would show up on the oscilloscope for a brief second and then return to noise. The amplitude of these peaks were then optimized by making adjustments to various parameters. Eventually, the peaks would remain on the oscilloscope for a few seconds, then a few minutes, and then they would stabilize. These pulses are termed ultrashort because the duration of each pulse only stretches a few hundred femtoseconds, where a femtosecond is 10^{-15} seconds.

With the mode-locked laser, the laser beam has the high intensity pulses required to produce the nonlinear optical processes within the PCF and produce the supercontinuum. Figure 13 displays the experimental setup for producing and monitoring the

supercontinuum. The spectrometers provided the primary source of data to measure the success of the supercontinuum process. Placing one spectrometer at the output of the Ti:sapphire laser and one at the output of the PCF, we were able to compare the spectra before and after the supercontinuum process to demonstrate its effect on broadening the wavelengths present.

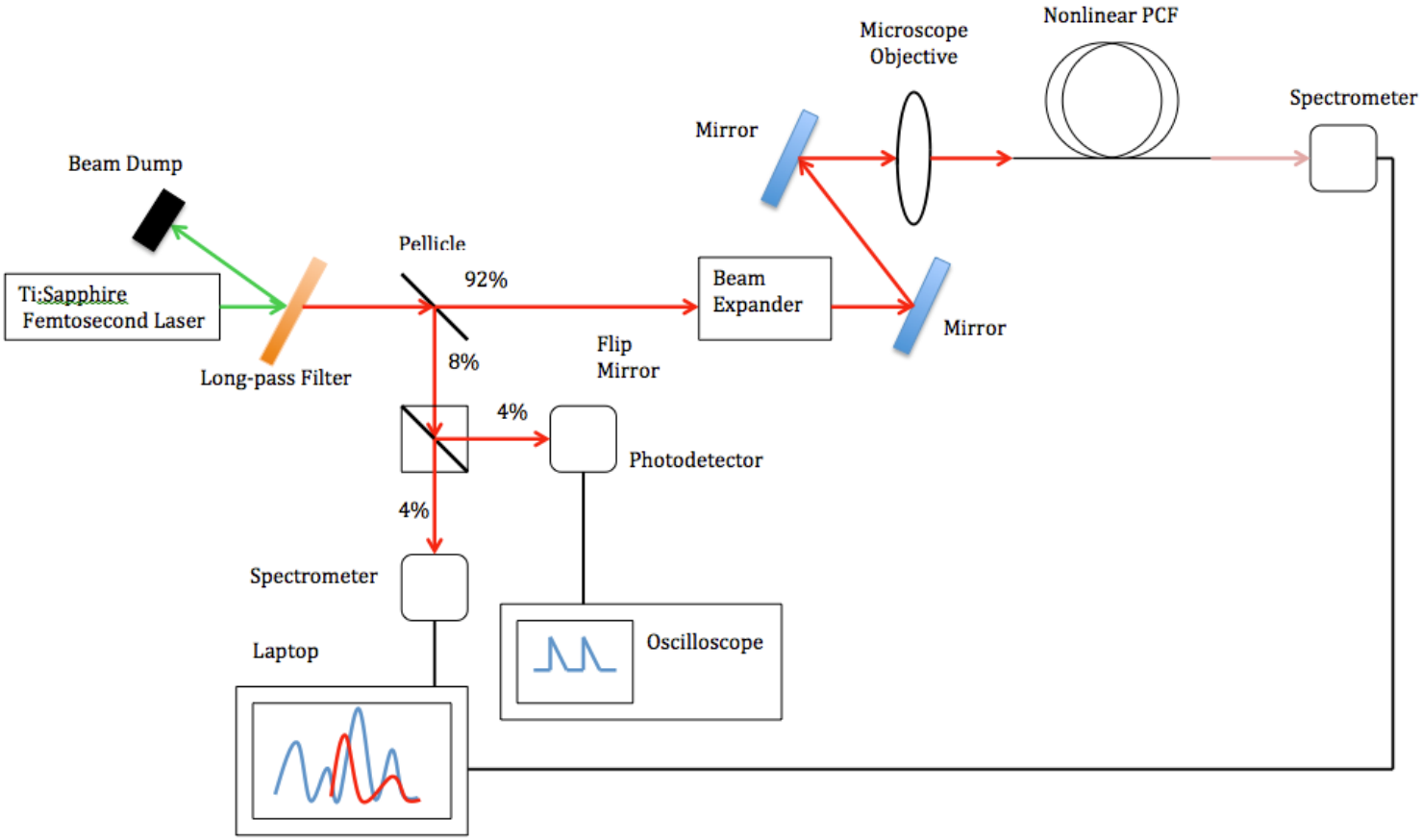

Figure 13: This is the setup that was used for observing supercontinuum. The beam expander and microscope objective focus the beam on the PCF core. The two spectrometers compare the input beam and the PCF output beam to observe the supercontinuum effect.

Photonic Crystal Fiber:

The first generated supercontinuum was generated in the late 1960s by Robert Alfano and Stanley Shapiro using a bulk BK7 glass (Dudley 2006). It broadened a 5mJ picosecond pulse at 530nm to a range of 400 to 700nm. However, this required a complex

process of manipulating spatial and temporal effects (Dudley 2006). "In contrast, supercontinuum generation in optical fibers involves purely temporal dynamical processes" (Dudley 2006). The optical fiber is manufactured to spatially maintain the beam while relying on the nonlinear temporal processes to broaden the spectrum. Therefore, optical fibers such as PCFs are more commonly used as the nonlinear medium in producing supercontinua.

Small-core PCFs are the preferred optical fiber for supercontinuum generation because of their design. The fiber's microstructure consists of a solid silica core of a few micrometers in diameter surrounded by air holes that run along the fiber's length in the cladding region, giving the fiber the effect of a solid glass cylinder suspended in air, as seen in Figure 14 (ThorLabs.com 2015). Thus, the refractive index of the core is higher than that of the air-filled cladding, causing the inserted beam to be internally reflected within the core with little loss. The fiber is not composed of crystals as the name might suggest, rather the air holes are arranged similar to a crystal (NKT Photonics 2009).

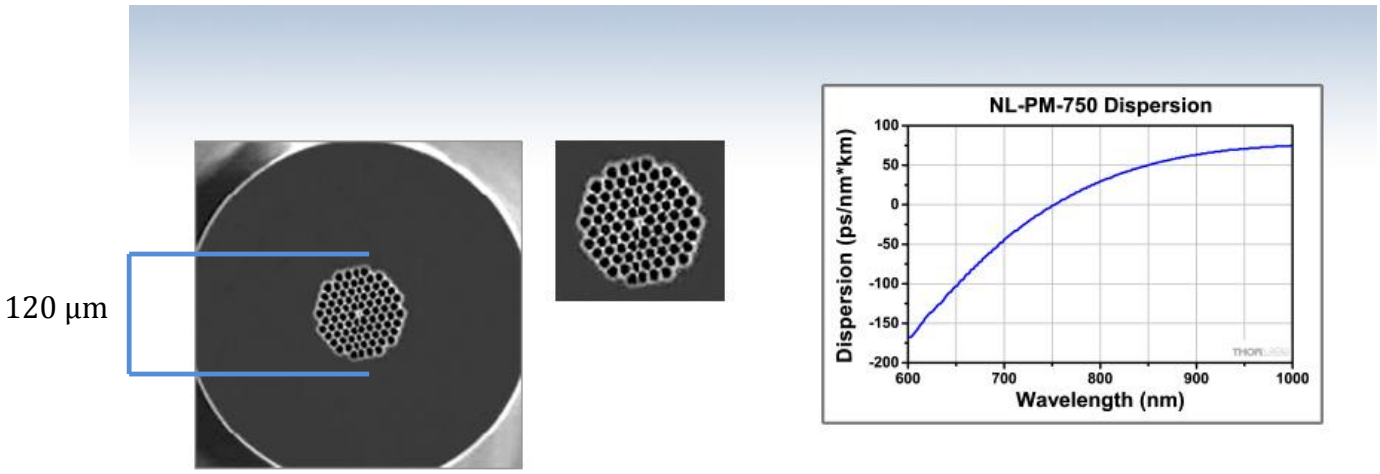

Figure 14: Left: the cross-section of a PCF. The center is a solid silica core, surrounded by the air hole cladding and an outer acrylic coating. Right: a graph of the anomalous dispersion of a PCF with a ZDW of 750 nm. Image Source: ThorLabs.com 2015.

This unique design is favorable for producing supercontinua. Dr. Jinendra Ranka's group at Bell Laboratories was the first to report the benefits of using air-cladding PCFs as opposed to solid optical fibers in 1999. Their study indicated that the high refractive-index difference between the air cladding and silica core and the tininess of the silica core allow for higher magnitude anomalous dispersion and group velocity dispersion (GVD) that covers the visible spectrum (Ranka, 1999). Anomalous dispersion means that the index of refraction of the material increases with an increase in wavelength, as is shown in the graph in Figure 14. The group velocity is the speed at which the envelope of the light wave travels through the fiber. The GVD is the dispersion that results from the group velocity's dependence on the light's frequency. The 2.4 μm diameter silica core allows zero dispersion wavelengths (ZDW) shorter than 1250nm, which is not achievable with conventional fibers (ThorLabs.com 2015). The ZDW is the wavelength at which no dispersion occurs within the fiber. Broader supercontinuum spectra occur with ZDW closer to the pump wavelength as will be explained in more depth later.

More specifically, it is the GVD that creates conditions favorable for supercontinua. The GVD causes the pulse to be stretched in time as the pulse propagates through the fiber. In other words, the frequencies are shifted out of phase. The dispersion characteristics and small core size allow for unique nonlinear and ultrashort pulse interactions at visible wavelengths (Ranka 1999). The combination of dispersion stretching the pulse in time and the nonlinear processes such as self-phase modulation (SPM) cause the supercontinuum to occur.

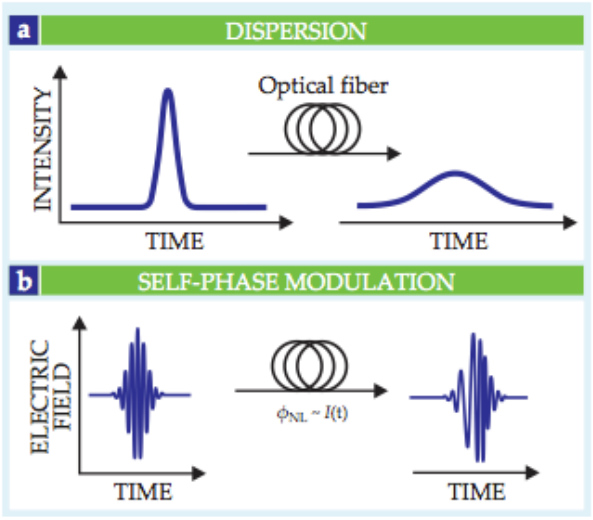

Figure 15: (a) The intensity of ultrashort pulses is concentrated in peaks. Dispersion causes the pulse to be temporally stretched. (b) The high intensity causes new frequencies to be made through SPM. Image Source: Dudley 2013.

The nonlinear optical processes are ignited by the intensity of the ultrashort pulses. The intensity of a laser beam is temporally distributed evenly throughout a continuous wave laser. On the other hand, mode-locked lasers send pulses with peaks where the intensity is concentrated in time as shown in Figure 15 a. This concentration of high intensity polarizes the dielectric PCF so that the induced polarization nonlinearly depends on the electric field of the laser beam (Dudley 2013). Thus, like with the Ti:sapphire crystal, through the optical Kerr effect, the refractive index is changed as a function of the intensity with respect to time.

The intensity-dependent index of refraction causes the instantaneous phase to behave nonlinearly as well. The phase equation gains a second nonlinear term, as indicated in blue in Equation 4 (Pe'er 2013).

$$\phi(t) = 2\pi f_0 t + k_0 n(I) L \tag{4}$$

Here, ϕ is the phase of the beam, f_0 is the central frequency of the beam, k_0 is the propagation constant in vacuum, n is the index of refraction(intensity dependent) and L is the thickness of the silica core. In the linear form, f_0 is a constant frequency in the phase shift. However, with the additional nonlinear term, the Kerr effect indicates that for these high intensity pulses, the index of refraction is dependent on intensity, which is dependent on time. This is more accurately depicted in Figure 16.

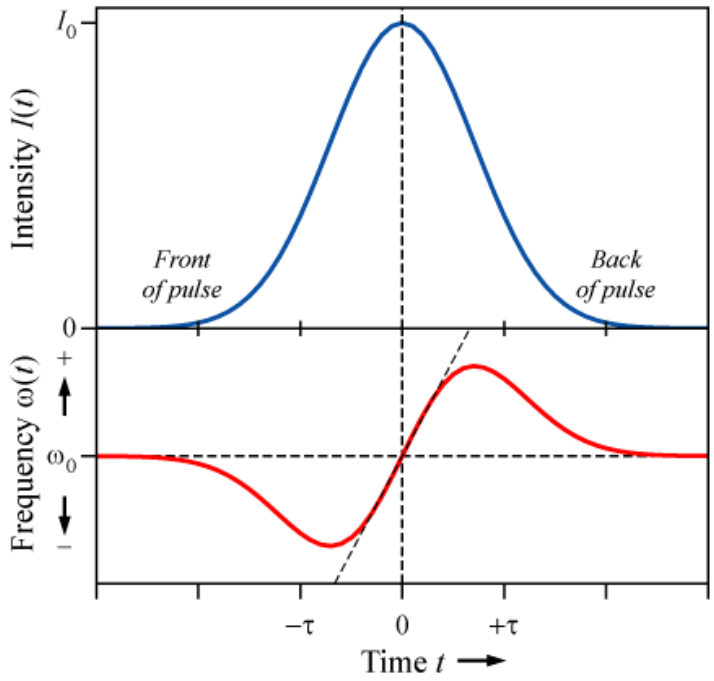

Figure 16: This figure demonstrates SPM. The blue curve represents the time-dependent intensity of the pulse. Due to the Kerr effect and the time-dependent intensity, the second term of Equation 4 creates a new frequency that changes with time, which is represented by the red curve. Image Source: http://upload.wikimedia.org/wikipedia/commons/9/9a/Self-phase-modulation.png.

Thus, the nonlinear term creates a new time-dependent frequency. The light pulse thus experiences a time-dependent phase shift known as SPM, creating new frequencies. "Specifically, it creates a temporally changing instantaneous frequency, or chirp, such that the lower frequencies appear on the pulse's leading edge with rising intensity and the

higher frequencies appear on the pulse's trailing edge with falling intensity" (Dudley 2013). This means that the red and infrared wavelengths are constructed at the beginning of the pulse while the blue and ultraviolet wavelengths are constructed at the end of the pulse. Together, the laser beam is spectrally broadened to encompass longer and shorter wavelengths.

In order to focus our laser beam, which is about 1200 μm in diameter onto the 2.8 μm diameter core, a beam expander and focusing lens had to be used. It is critical that the beam be reduced to a size as close to the fiber core size as possible without exceeding it. If the beam is focused too tightly, the beam may enter the fiber at too steep of an angle and diffract through the silica core. If it is not focused enough, part of the beam is lost and does not go through the nonlinear processes. Thus, the magnification power of the lens affects the spectrum results.

Contrary to what seems initially logical, the beam expander helps to focus the beam more intensely. According to the equation for focal beam width, $w_{theoretical}$, as shown in Equation 5, the focused beam width is inversely related to w_0, the beam width before entering the focusing lens (Crist, 2012). For the purposes of this experiment, the beam width was accepted as the diameter of the beam at 13.5% of its peak intensity, also known as $1/e^2$, which is widely used by optical physicists for measuring beam diameter. This was measured using the beam map.

$$w_{theoretical} = \frac{\lambda F}{\pi w_0} \tag{5}$$

Here, λ is the wavelength of the laser beam, 810 nm, and F is the focal length of the focusing lens. Thus, the wider the initial beam, the tighter the focused beam width will be. We used an M-65X focusing lens with a focal length of 2.5 mm. Originally the beam's

diameter was 630 ± 20 μm, which gave a focused beam diameter of 4.1 ± 0.3 μm, compared to the 2.40 μm diameter core of the PCF. By using a four times beam expander, the beam was expanded to 2520 ± 20 μm in diameter and the focused beam diameter was thus reduced to 1.02 ± 0.04 μm, which was within the PCF core limit.

A Z-mirror setup was again used to ensure that the laser beam entered the focusing lens directly in the center. To focus this beam on the 2.4 μm core of the PCF required immense precision in aligning the fiber with the focusing lens and clarity of the PCF. A fiber chuck was mounted in a positioner that could translate the chuck horizontally and vertically using dials. Moving the fiber forward or backward to achieve the correct distance from the lens required carefully nudging the positioner forward or backward.

The fiber itself required constant maintenance to ensure clarity of the exposed face. Any dust or scratches on the exposed surface of the silica core could affect the supercontinuum. Just inserting the fiber into the chuck, which involves sliding the fiber through an aperture, could damage the fiber. Since the fiber is too small and fragile to be cleaned using chemicals or wipes, the damaged fiber face has to be sliced off. This then provides a fresh exposed surface free of debris or scratches.

The fiber was inserted into the chuck before cutting because this process damages the fiber to begin with. The coating around the fiber has to be stripped by using precision wire strippers. Yet, the coating had to be cut about 8 mm out from the tip to provide enough length of exposed core for cutting. The actual silica core of the fiber is only 105 μm in diameter but the smallest size on the wire strippers was 125 μm, so an extra squeeze was used to make a deep enough cut through the coating without damaging the core. Bracing the length of the fiber against my forefinger, a diamond edged scribe was used to

tap the edge of the fiber about 5 mm from the coating, ensuring that the scribe's flat edge hit perpendicular to the length of the fiber. By then taping the damaged fiber tip to the edge of a table, the fiber could be carefully bent back to snap itself cleanly along the scribed edge. Since the beam is focused, it is very intense at the focus and could melt the outer coating, creating smoke that could damage the fiber core. Thus, leaving 5 mm of fiber exposed allows for the laser beam to focus on the fiber core without striking the coating. This process was repeated for both ends of the fiber.

The fiber was then carefully positioned near the focus of the focusing lens and aligned using the chuck positioner. Alignment was assured when the fiber began to glow along its length. This showed that the light was traveling through the air holes and propagating along its length. The fiber was then adjusted slightly so that the beam became contained within the silica core and the glow disappeared. However, the light coming out of the other end of the fiber was not a laser beam, but rather a point source of light. In order to measure the wavelengths present in the output beam, another focusing lens was used inversely to expand the beam. Another spectrometer was then set in front of the beam and connected to the same laptop as the first spectrometer and compared, as displayed in Figure 13.

Frequency-Resolved Optical Gating:

In addition to observing how different variables affect the breadth of the supercontinuum spectrum, this project also hopes to prove that the supercontinuum process is partially due to self-phase modulation (SPM). This requires measuring the ultrashort pulses temporally. However, to measure any temporal event, a shorter event is required to compare it to. Femtosecond pulses are the shortest known events that have

been produced, so it seems impossible to try to measure them. Thankfully, Rick Trebino devised a method to use the ultrashort pulse to measure itself. This method is realized in the Frequency-Resolved Optical Gating (FROG) device, which can analyze the pulses before and after the fiber to demonstrate the effect the SPM process has. Comparing the FROG trace of the laser beam before the PCF to that of the laser output by the PCF would demonstrate the occurrence of SPM within the PCF.

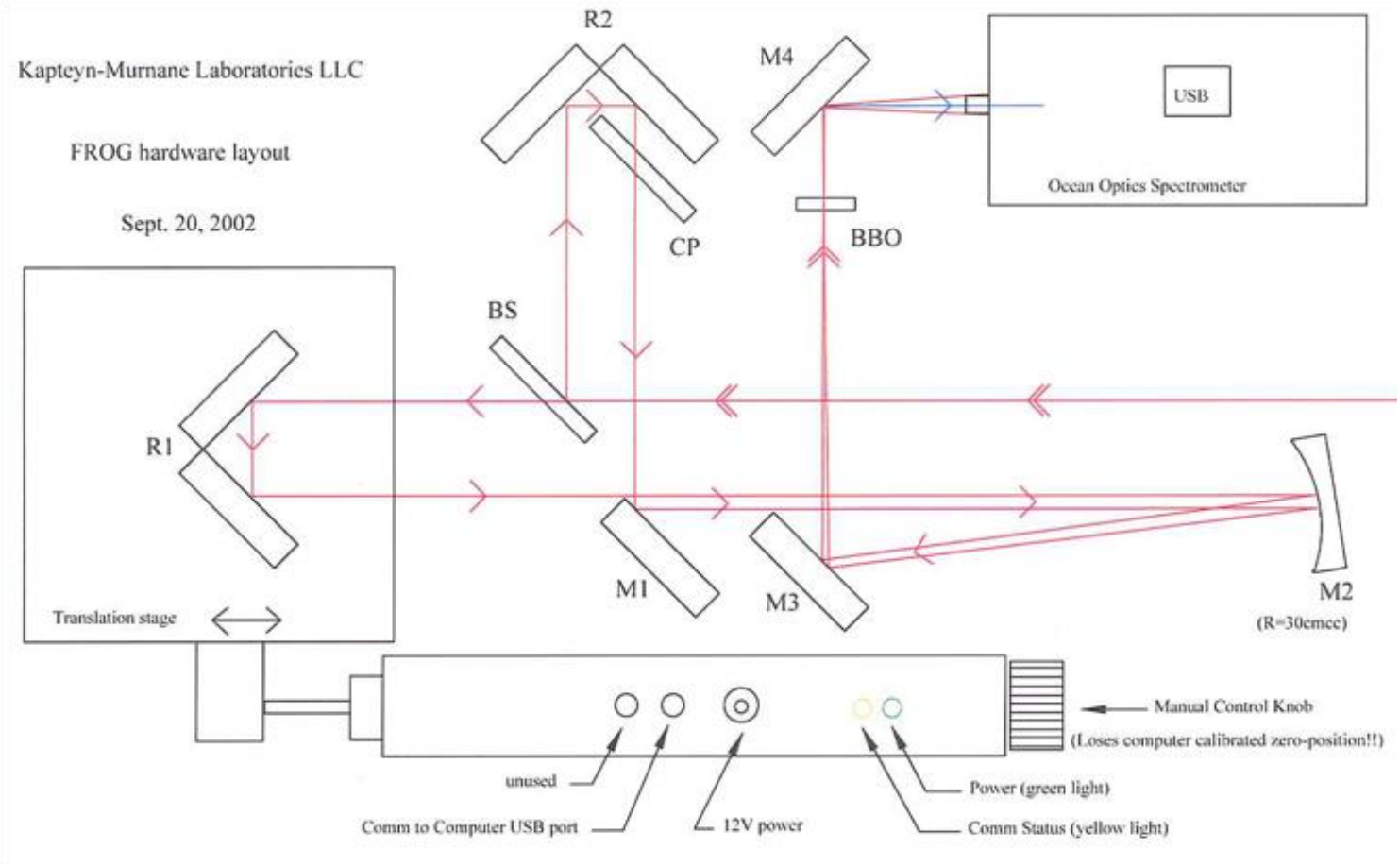

Figure 17: This diagram demonstrates how the FROG device splits the laser beam to reference itself for measurement of time delay. The beam enters the device from the left. BS is a beam splitter that sends the reference pulse to R2, and the gated pulse to R1. R1 is on a translation stage activated by a step motor. Both pulses then meet up at M2, are sent through the BBO crystal and enter the spectrometer. Image Source: Kapteyn-Murnane 2002.

Initially, the device splits an incoming pulse into two pulses: a reference pulse and a gated pulse. The gated pulse travels an adjustable distance using two reflectors (R1) on a stage that is translated by a step motor. By adjusting the distance traveled, the pulses can be set out of phase by a few micrometers, which is the equivalent of delaying the pulse by femtoseconds. These two pulses then converge on a Barium Borate (BBO) crystal. This nonlinear optical crystal causes second harmonic generation (SHG) of any phase-matched light source within a certain wavelength range. When the reference pulse and gated pulse first converge on the BBO crystal, two dots appear, one on either side of the spectrometer input due to their reflection off of M4. However, when these two light sources are overlapped in time and space, the BBO crystal outputs a light of half the wavelength between the two dots, or twice the frequency, which in our case is 405nm or blue. This effect is used to determine the time delay of the gated pulse from the reference pulse.

In order to align the two pulses within the BBO crystal, the step motor had to be manually controlled. A white card was placed in front of the spectrometer to watch the two dots that straddle the spectrometer aperture. Starting with the step motor arm completely withdrawn (R1 closest to the laser beam input), the stage was slowly incremented forward, watching for a blue dot to appear between the two dots. Once this location was found small increments were made to maximize the intensity of the blue dot. The spectrometer was then hooked up to a laptop using Oceanview software for more precise alignment. Although the FROG software has a program for this purpose, it was not as sensitive as the Oceanview spectrometer software. Thus, M1 and M3 were rotated slightly to maximize intensity of 405nm on the spectrometer. Tampering with any of the other mirrors or reflectors would require recalibration in factory, so they were left alone.

The device then uses this time delay along with second harmonic generation (SHG) to compare the two pulses and measure the wavelengths present with the spectrometer. By having one pulse as a reference, the device can sweep through it in increments of femtoseconds using the mirror on the step motor to change the distance the gated pulse must travel to reach the SHG crystal. This effectively moves the delay beam out of phase of the reference beam, which allows the FROG to compare the beams and measure the wavelength as the pulse translates in time. In this way, it maps out the wavelengths that are present in the pulse in relation to time, as seen in Figure 18. This device can hence detect if certain wavelengths are leading the pulse or trailing the pulse.

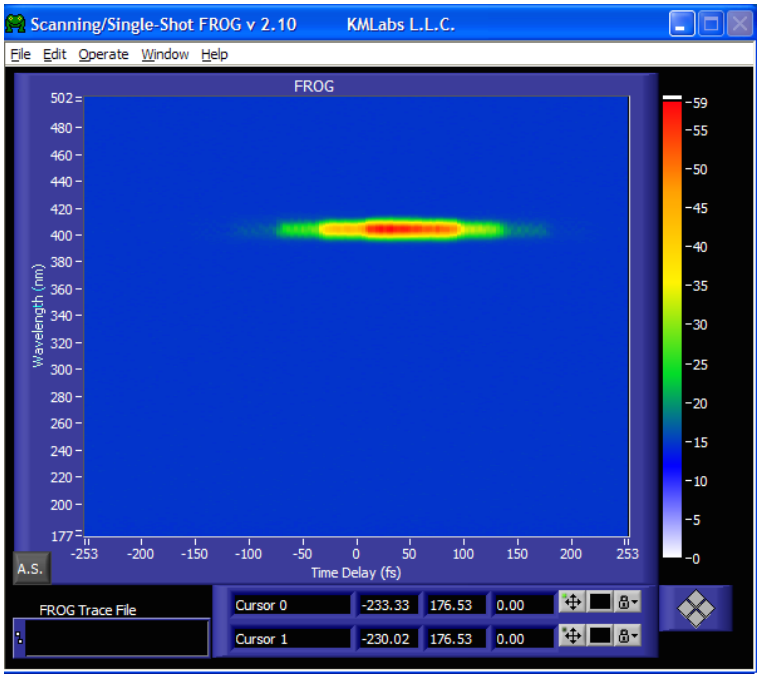

Figure 18: This is a FROG trace of the ultrashort pulse before it enters the PCF. The x-axis represents the time delay of the pulse and the y-axis represents the wavelengths present at that time in the pulse. The colors represent the intensity of the wavelength, with red being most intense and white not present at all. The blue is a result of the spectrometer measuring the natural light of the room.

In order to analyze the pulse effectively, the entire laser beam had to be sent to the FROG. However, we wanted to be able to measure the pulse on the FROG and send the

pulse to the PCF without requiring a large amount of realignment of mirrors. Thus, we decided to use a flip mirror that would redirect the beam at an angle while obstructing its path, and allow the beam to pass unaffected when the mirror is flipped down, out of the path of the laser beam as depicted in Figure 19. The following two mirrors are set in a z-mirror formation. This setup allows the beam to be set at the exact height and direction necessary to enter the FROG perpendicularly to its surface.

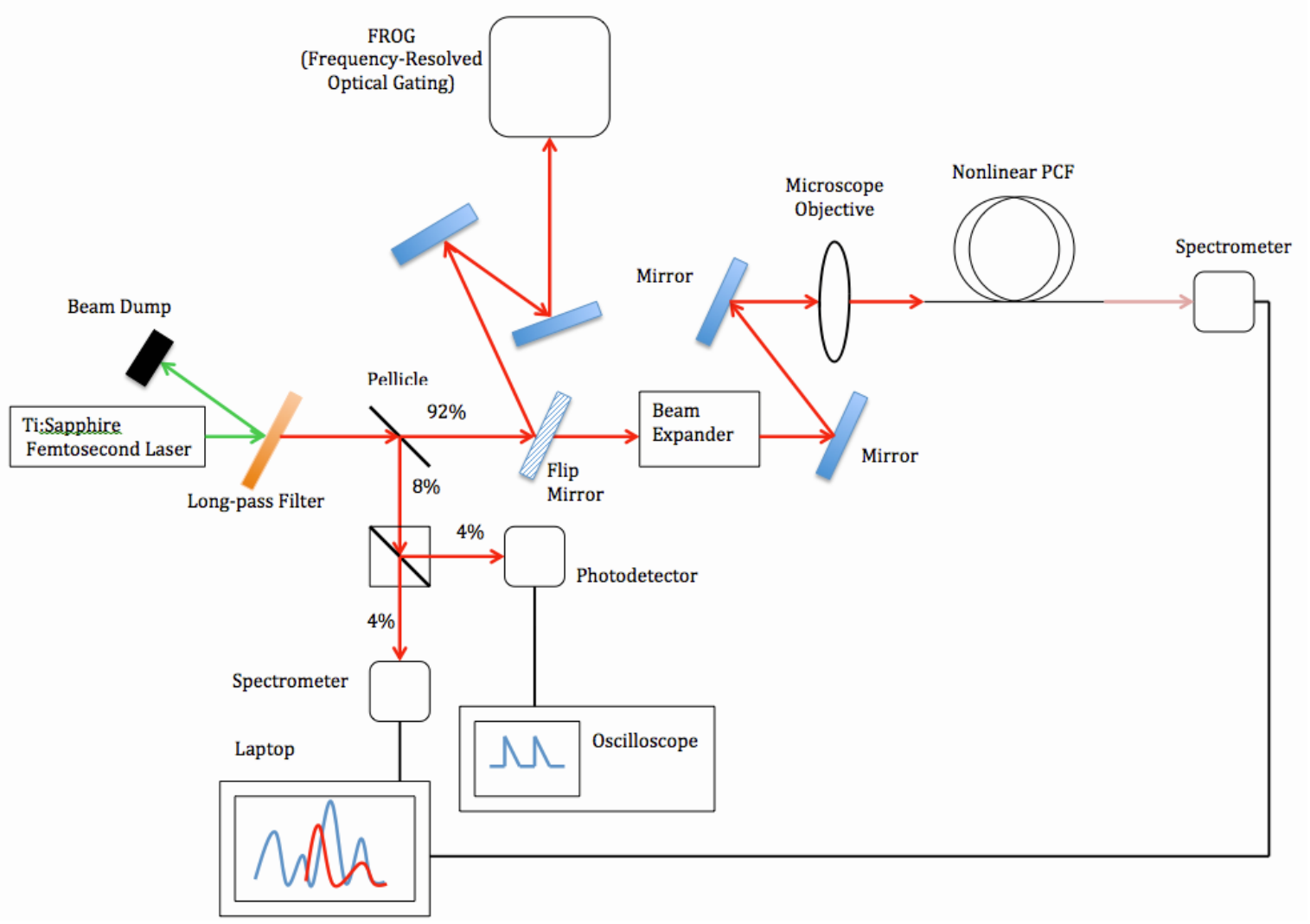

Figure 19: The FROG device was added to the setup using a flip mirror so that the supercontinuum setup would not have to be sacrificed to access the laser. The z-mirror aims the laser to enter the FROG at the correct height and angle.

Analyzing the pulse straight from the Ti:sapphire laser, the FROG can determine the duration of the pulse. According to the FROG device's measurements, this laser produces about a 300 ± 50 femtosecond long pulse, as seen in Figure 18. Since it was measured before the fiber, the pulse is only a horizontal dash, meaning the short wavelengths (the blues) and the long wavelengths (the reds) are both happening at relatively the same time within the pulse. Note that since the device uses SHG to analyze the pulse, the wavelengths detected are half of their actual value in the pulse, meaning that the pulse actually had wavelengths around 820nm.

Theoretically, if the FROG were to measure the output of the PCF, the FROG could uniquely determine if self-phase modulation had occurred. According to John M. Dudley and Goëry Genty, the self-phase modulation creates a phase shift that changes in time with the intensity of the pulse, which generates new frequencies, forming a changing chirp in the pulse (Dudley 2013). This is how the new wavelengths are formed that produce the broadened spectrum. The longer wavelengths are formed toward the front of the pulse and the shorter wavelengths are formed towards the end of the pulse due to the chirp.

A positive chirp would show up on a frequency vs. time graph as a diagonal line from lower left to upper right, considering the longer wavelengths start earlier in the pulse and the shorter wavelengths occur later on in the pulse (Trebino 2015). In the case of self phase modulation, the chirp is changing with time so instead of a diagonal line, we get an "S" shape. At the beginning of the pulse, there should be a concave up curve, where the lower frequencies are present. Then, on the trailing edge of the pulse, the higher frequencies are present, resulting in a concave down curve on the frequency vs. time graph.

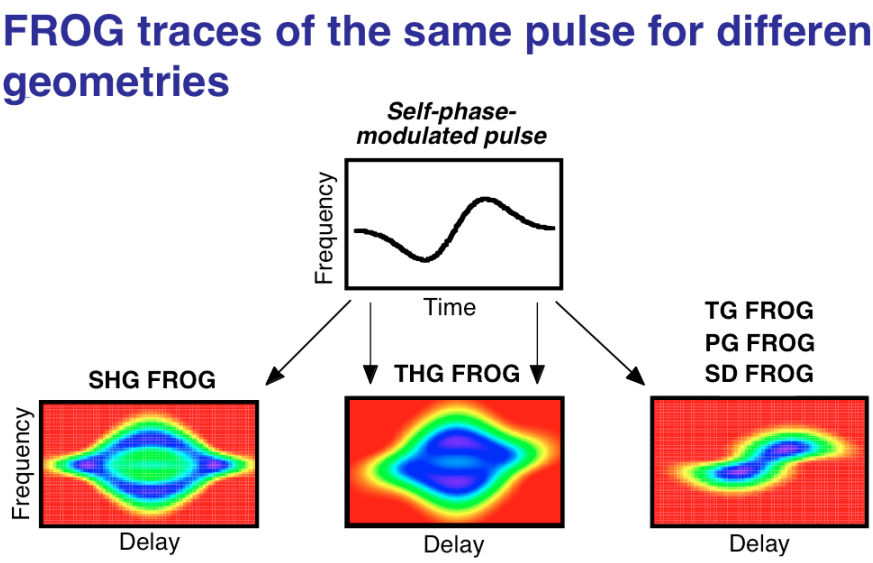

Figure 20: This displays FROG traces of a SPM pulse. Different FROGs use different nonlinear optical devices or methods to measure the pulses such as Third Harmonic Generation (THG), Transient Grating (TG), Polarization Gate (PG), and Self-Diffraction (SD). Our FROG uses SHG. Note that these graphs are frequency vs. time and not wavelength vs. time as in Figure 18. Image Source: Trebino 2015.

Rick Trebino shows what the FROG would show if it analyzed a pulse that had undergone self phase modulation. Our FROG uses SHG as mentioned above, so we would expect a FROG trace similar to the one on the left if we were to analyze the beam exiting the PCF. There are other types of FROGs, made from different nonlinear optical devices or methods to measure the pulses such as Third Harmonic Generation (THG), Transient Grating (TG), Polarization Gate (PG), Self-Diffraction (SD), and SHG, which is the FROG we used. Trebino mentions that the TG, PG, and SD FROGs have a trace that is intuitive, as we would expect, and that the SHG FROG has a trace that is least intuitive (Trebino 2015). The SHG FROG traces are symmetrical traces due to the effect of using SHG to measure the pulse.

Analysis:

The extent of spectral broadening depends on the relationship between the wavelength of the pump laser beam and the zero dispersion wavelength (ZDW) of the PCF. The Ti:sapphire laser was mode-locked at 810±20nm and the PCF that was implemented had a ZDW of 800nm. The relationship can generally be described by Table 1. In our case, the pump wavelength was almost at the ZDW, which results in an irregular, medium-wide spectrum with a dip at the ZDW.

Pump Wavelength	Output Spectrum
Below the zero dispersion wavelength	Stable, smooth and narrow spectrum
At the zero dispersion wavelength	Irregular, medium-wide and with a dip at the zero-dispersion wavelength
Above the zero dispersion wavelength	Irregular and wide spectrum

Table 1: ThorLabs, the manufacturer of the PCF describes how the relationship between pump wavelength and ZDW affects the output spectrum. Image Source: ThorLabs.com 2015.

The expected spectrum breadth is not specified in this table, but the manufacturers refer to a supplementary document on the application of PCFs to produce supercontinuum. This document reported spectral results of using various PCFs. Although it did not report any results using an 800nm ZDW PCF with an 810nm pumping wavelength, the document gave comparative results. Figure 21 demonstrates how various pump wavelengths affect the output spectrum using the same PCF with the same ZDW.

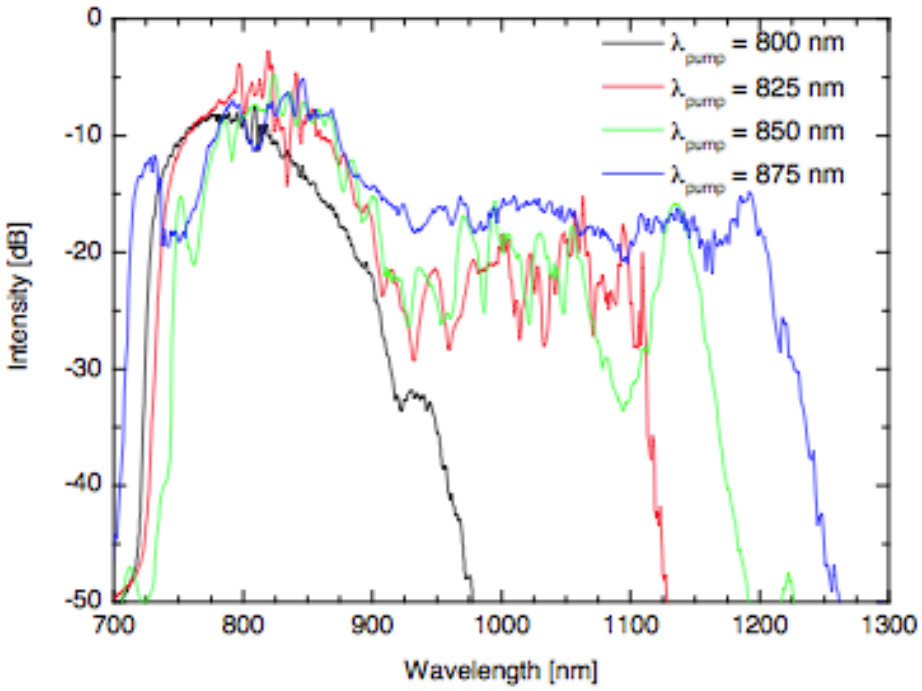

Figure 21: The resulting supercontinuum of various pumping wavelengths sent through a PCF with a ZDW of about 900nm. The fiber is pumped by 100 fs pulses with a repetition rate of 76 MHz at a coupled average pumping power of 50 mW. Image Source: NKT Photonics 2009.

The pumping wavelengths are all below the ZDW. As the pumping wavelength approaches the ZDW the spectrum broadens to about 500nm wide at -20 dB when the discrepancy between ZDW and pumping wavelength is only 25nm. Thus, since the difference between pumping wavelength and ZDW was only 10nm for our 800nm ZDW PCF, we would expect optimal conditions for broadening the spectrum.

The resulting spectrograph comparing the spectrum of the input Ti:sapphire laser beam and the beam output by the PCF is displayed in Figure 22.

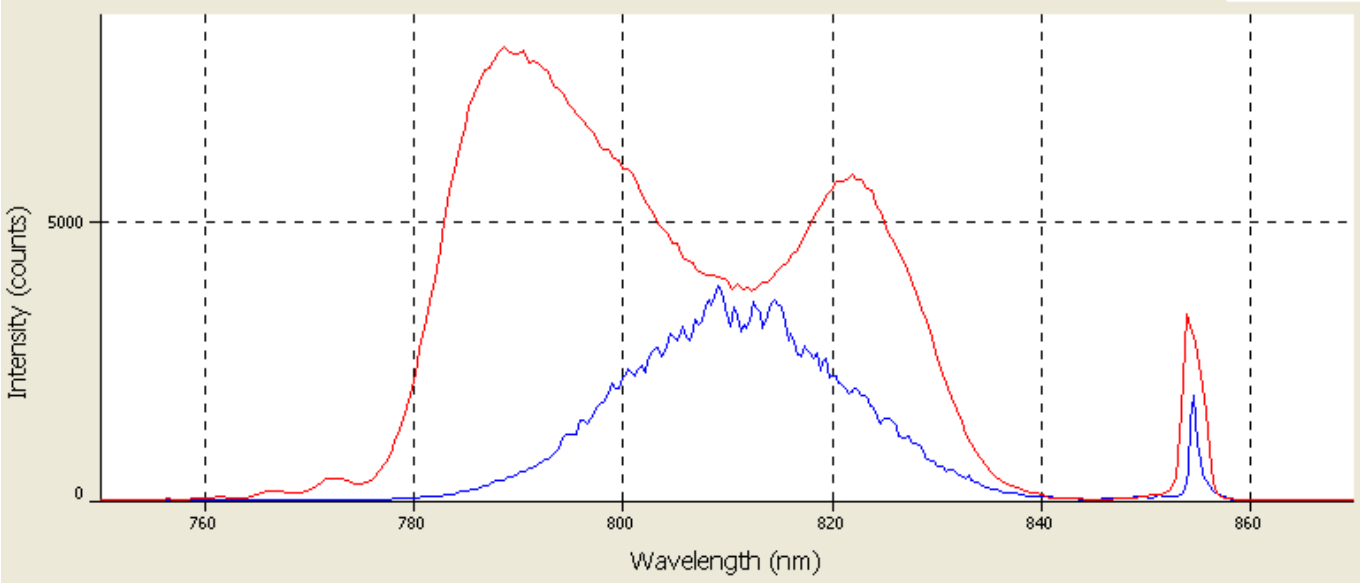

Figure 22: The spectrometer measures the wavelengths present in the Ti:Sapphire laser beam (blue) and the laser beam with a broadened spectrum as it exits the PCF (red).

The input beam had a power of 0.51 W after the samplers and the beam output by the PCF was 0.04 W. Here, we can see the dip at about 810nm, which is close to the ZDW as predicted by Table 1. Looking at the width of both spectral peaks, the input had a spectral width of about 40±5nm (790nm-830nm) and the output width was 70±5nm (765nm-835nm). As for the peak at 855 nm, this most likely indicates that part of the beam found an alternate route through the laser to produce this extra wavelength.

These results may be misleading because the intensity in Figure 22 is measured in counts. The count rate can be set manually for each spectrometer. However, even when both spectrometers were set to the same count rate, the intensity of the output of the PCF (red) was measured to be significantly greater than that of the input (blue), even though the opposite was true due to the negligible power output. The red curve spectrometer had a saturation threshold at 15,000 counts, while the blue curve spectrometer had a saturation threshold at 4,000 counts. This indicates that the count is arbitrary between

spectrometers because the red curve spectrometer is more sensitive. For the purposes of Figure 22, the count rate of the red curve was significantly decreased so that the curve shape could be observed and compared to the blue curve.

Since the graph in Figure 21 measures intensity in logarithmic scale, it is not accurate to compare it to Figure 22, a linear graph, as far as results. If Figure 22 were set to a logarithmic scale, with intensity in dB, the lower intensity wavelengths would be more prominent. To get a more accurate account of the wavelengths present at lower intensities, Figure 23 was taken at maximum count rates for each spectrometer, causing a saturation threshold for the blue curve. Here, the red curve demonstrates that the supercontinuum spectrum covered 750 nm to 860 nm.

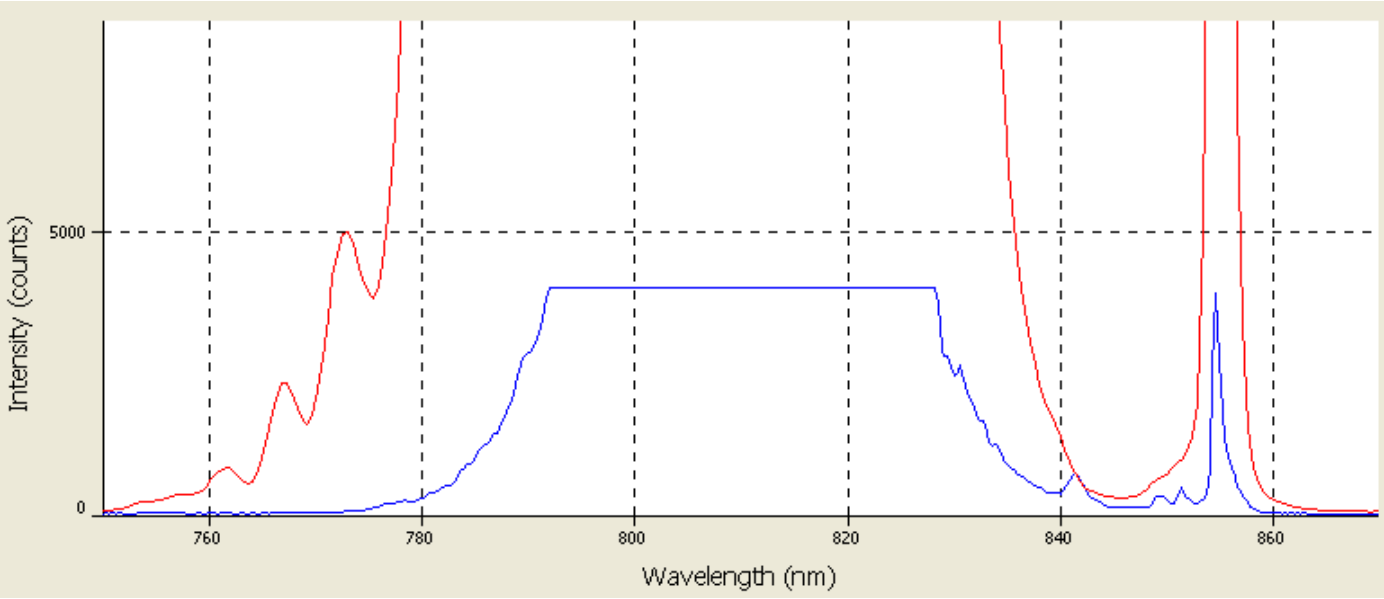

Figure 23: This is a spectrograph of the laser beam before the PCF (blue) and after the PCF (red) with high count rate. The blue curve has a saturation threshold at 4,000 counts.

Also, we were unable to retrieve a FROG trace of the output spectrum because the output pulse was too weak at only 0.04 W in power. Since the output from the PCF was just a point source of light and not a propagating beam, the output laser could not propagate

through the FROG apparatus as needed. To take a FROG trace, the output beam would have to be split, delaying one of the beams and comparing both of them. Without a propagating pulse, this could not be measured. Rick Trebino mentions an alternative pulse analysis device, Temporal Analysis by Dispersing a Pair Of Light E-fields (TADPOLE), which is used to measure pulses as weak as 42 $*10^{-21}$ joules, however this device was not accessible to us (Trebino 2015).

The pump power of the Verdi laser was varied to see how it affected the spectrum of the supercontinuum. The theory was that perhaps a higher input power would produce a more intense beam that would undergo the Kerr effect and SPM more intensely to create a broader supercontinuum spectrum. This test was performed in the afternoon, after the Ti:sapphire laser beam achieved a constant power. The pump power started at 5.00 W and was then decreased by increments of 0.10 W until it stopped mode-locking, observing changes in the supercontinuum spectrum, as seen in Table 2. The same was done increasing by 0.10 W until 6.00 W, at which point I decided to stop for safety of the equipment. These results can be seen in Table 3. They both imply that changing the pump power increases the intensity of the wavelengths present, but does not assist the supercontinuum process in producing more wavelengths.

Pump Power (W)	4.70-4.30	4.30-4.00W	4.00-2.40
Spectrum Description	Slight increase in intensity, no spectral broadening.	Spectrum decreased back to original state at 5.00 W, no spectral broadening	Intensity and spectrum decreased until stopped mode-locking at 2.40 W

Table 2: The Verdi pump power was decreased by increments of 0.10 W and the supercontinuum spectrum was observed.

Pump Power (W)	5.10-5.50	5.50-5.70W	5.70-6.00
Spectrum Description	Slight increase in intensity, no spectral broadening.	Spectrum decreased back to original state at 5.00 W, no spectral broadening	Intensity and spectrum decreased

Table 3: The Verdi pump power was increased by increments of 0.10 W and the supercontinuum spectrum was observed.

Note that these are results of one instance on one day and so may not accurately reflect the relationship between pump power and spectral range. The Ti:sapphire beam power varied from day to day because adjustments had to be made to mirrors to keep the laser mode-locked and lasing. The Ti:sapphire beam power varied over the course of this research from 0.50 W to 0.90 W in the continuous wave state. Mode-locking usually produced a pulsing beam with power ranging from 0.30 W to 0.50 W. Additionally, the Ti:Sapphire beam power varied from hour to hour as the laser warmed up. When turning on the Verdi laser, the apparatus had to be left alone for the first few hours before it produced a laser beam. Even just optimizing the positioning of the high reflector and output coupler, the output power would not reach 0.40 W until a few hours later. This was probably due to the change in temperature of the room throughout the day, as can be seen in Table 4. Although the crystal is cooled by a water coolant, the precision of the mirrors is so critical that temperature changes would cause the table to expand and contract enough that the mirrors became misaligned.

Time of Day	8:40 AM	10:10 AM	10:30 AM	11:14AM	11:50PM	1:00PM
Description	turned on Verdi	started lasing	lasing	mode-locked	mode-locked	mode-locked
Power (W)	0.0	0.05	0.17	0.33	0.37	0.39

Table 4: This table demonstrates the optimal output power of the Ti:sapphire laser throughout the day with just adjusting the output coupler and high reflector. Beam power was measured after the samplers and before the focusing lens.

Another important aspect to consider in analyzing Tables 2 and 3 is how the Verdi pump power affects the Ti:sapphire beam power. It is the Ti:sapphire beam's intensity that is directly applied to the PCF to create the supercontinuum. Similar to Table 2, the Verdi pump power was decreased by increments of 0.10 W. These results are displayed in Table 5. Unfortunately, this test was not performed incrementing the pump power. Table 5 implies that the Ti:sapphire beam power is relatively constant until it is decreased below 4.50 W.

Pump Power (W)	5.00	4.90	4.80	4.70	4.60	4.50	4.40	4.30	4.20	4.10
Ti:sapphire Power (W)	0.46	0.45	0.46	0.44	0.43	0.44-0.36	0.38-0.26	0.24-0.22	0.24-0.19	0.15-0.16

Table 5: The Verdi pump power was decreased by increments of 0.10 W and the Ti:sapphire power was measured after the samplers.

Future Research:

Since the spectrograph results do not cover the visible spectrum or even reach 600 nm, there is room for improvement. More importantly, in order to take a FROG trace of the PCF output beam, the beam needs more power, much of which was lost traveling through the PCF. This trace would demonstrate the SPM that occurs within the fiber to produce the supercontinuum. The most likely solution to producing a more powerful output beam would mean better alignment of the focused laser beam with the PCF. After data was taken, attempts were made to improve the output power and broaden the spectrum. However,

there was not enough time to align the beam with the PCF adequately to achieve a supercontinuum or even produce an output beam. It would be beneficial for future researchers to align the beam with these additional changes to see how effective they were in improving the beam.

The laser beam's propagation is critical in alignment so the Z-mirrors were extended to increase precision. By increasing the distance between the Z-mirrors, the constant height of the propagating beam can be ensured at a greater degree. This then allows the second mirror to control the direction of the beam being reflected more precisely.

To ensure that the beam was propagating desirably, a beam map CCD camera and power meter were used at various locations. The beam was observed right after the first Z-mirror, after the lens, and after an empty chuck (fiber removed). The results are represented below in Figures 24-26. The top right shows the intensity of the beam in colors ranging from red, yellow, green, and blue with red being the most intense. The lower left and right graphs show a cross section of the 3D intensity graph. In other words, it shows the intensity of a slice of the beam in the x and y direction.

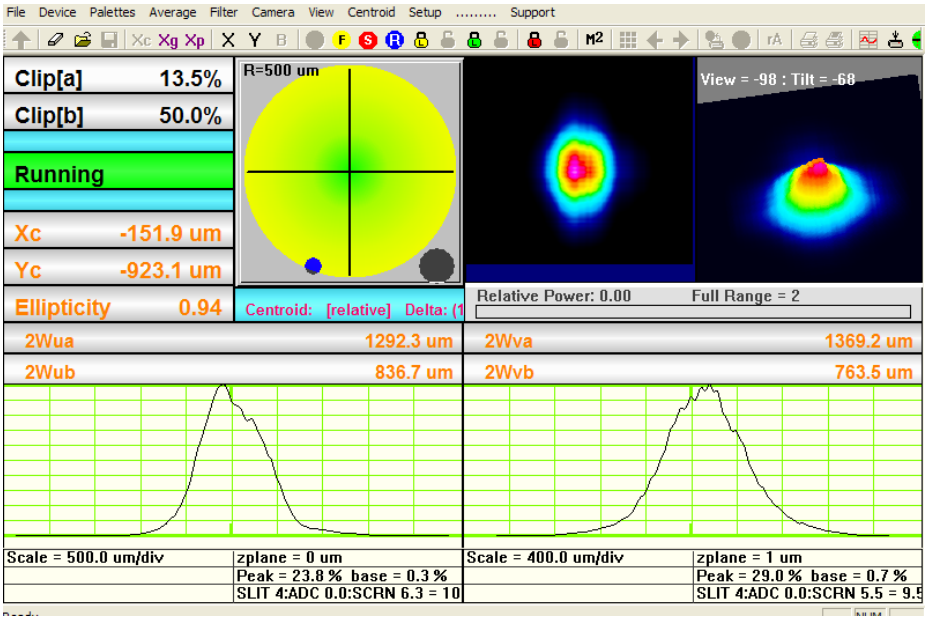

Figure 24: Beam map after first Z-mirror. Power was 0.20±0.01W.

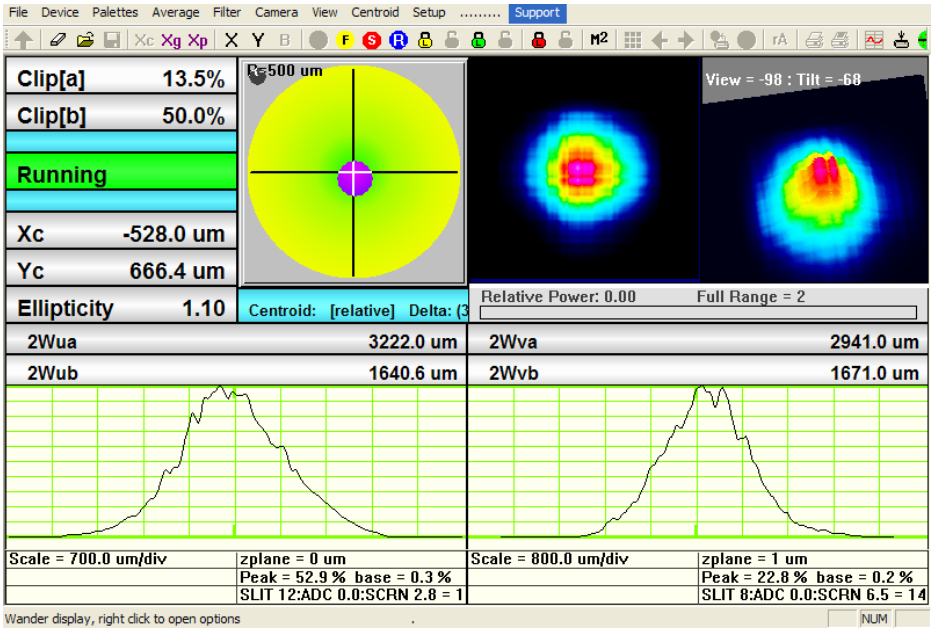

Figure 25: Beam map after lens. Power was 0.15±0.01W.

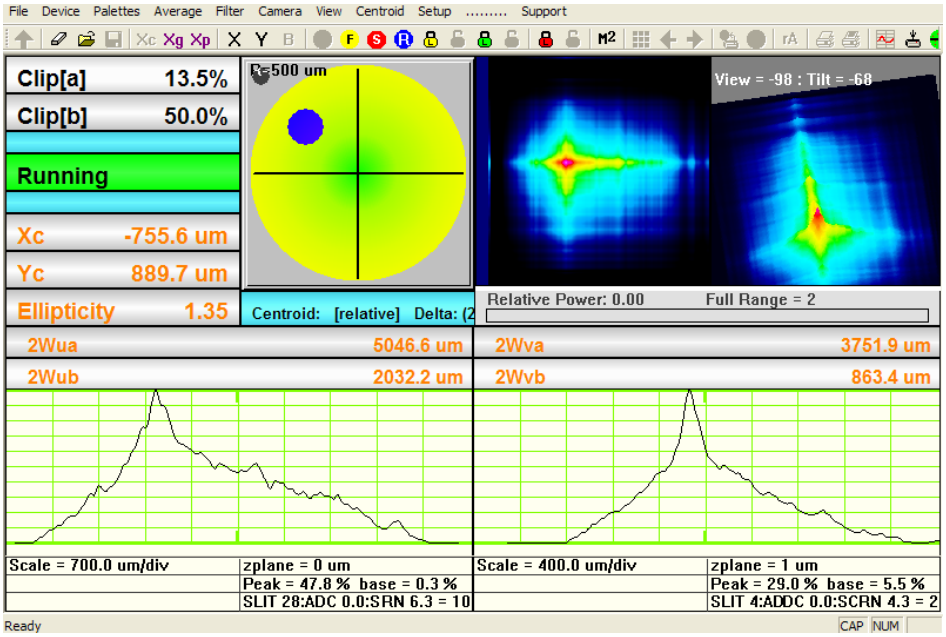

Figure 26: Beam map after the chuck. Power was 0±0.01W.

These maps explain the state of the beam at each location. An ideal beam has a Gaussian shape with the highest intensity at the center of the beam, radially decreasing in intensity outward from the center. The ellipticity measures how circular the beam is, thus it is ideal to have an ellipticity of 1. Right after the first Z-mirror the beam is quite ideal with its shape and an ellipticity of 0.94 (Figure 24). After the lens, the beam still has a Gaussian shape, but is not as smooth and has lost 0.05W of power. This shows that the lens might not be as clean or efficient as it could be. Finally, looking at the beam map after the chuck, the beam is distorted because it was focused on the front of the chuck to fit the small diameter of the PCF. The beam then expanded from the focus as it traveled to the other end of the chuck so some of the beam is cut off. The beam did not even have enough power to be registered by the power meter. This demonstrates the importance that the beam is contained within the PCF as it propagates.

Alignment of the PCF was improved by incorporating an XYZ stage to provide full manipulation of the positioning of the fiber on the micron level. Once inserted, the fiber

could be shifted left, right, up, down, forward, and backward at micrometer increments using the respective dials. Precision was improved most significantly in the forward and backward translation, which is important in positioning the fiber at the focus of the lens.

Also, the length of the fiber can cause complications as well. If the beam travels too long within the PCF, the nonlinear processes may become unstable. Trying smaller lengths of fiber could provide better results. Since the ends of the fiber are so crucial to the outcome of the supercontinuum, it was also beneficial to re-cleave the end of the fibers and make sure they are clear of dust, debris or cracks. Thus, the PCF was cut to 125mm and placed in the XYZ stage to achieve better results. There was not enough time to align the shortened PCF and achieve supercontinuum.

Just as the PCF's clarity is crucial to the supercontinuum success, the Ti:sapphire crystal must also be cleaned regularly. The crystal was wiped with methanol on an optics applicator swab once every couple months while the mirrors were left alone. However, when Dr. Greg Taft observed the laser, he suggested cleaning the crystal weekly. He also noticed scratches on the inner cavity mirrors. Replacing these mirrors would improve the power of the laser and make mode-locking easier. Another factor would be trying the 750 ZDW PCF that was also purchased to verify the relation of pumping wavelength and ZDW. According to Table 1, since the pumping wavelength would be above the ZDW, we would expect a wider, more irregular spectrum.

Acknowledgements:

I would like to thank Dr. Dean Langley for his constant support, patience, and guidance in this thesis project. His knowledge on troubleshooting with lasers was invaluable in constructing the Ti:sapphire laser. Also, much gratitude is expressed to Dr. Todd Johnson and Dr. Adam Whitten along with Dr. Langley for critiquing my thesis and providing feedback. Dr. Johnson also assisted by providing helpful advice on positioning the PCF based on his past work with optical fiber. Finally, I thank Dr. Greg Taft whose research on constructing Ti:sapphire lasers and his connection to Kapteyn-Murnane Laboratories Inc., the manufacturer of the FROG, proved to be a helpful resource in this project.

References:

Crist, Jordan, and Chad Nelson. *Predicting Laser Beam Charactersitics*. Coherent, Inc. 2012. 37. PDF.

Dudley, John M., and Goëry Genty. "Supercontinuum light." *Physics Today*. July 2013. 29-31. PDF.

Dudley, Jon M., Goëry Genty, and Stéphane Coen. *Supercontinuum generation in photonic crystal fiber*. Reviews of Modern Physics. American Physical Society. 2006. 1135-1141. Web.

Kapteyn, Henry C. and Margaret Murnane. *Mode-Locked Ti:Sapphire Laser*. Rev 1.6. Washington State University Department of Physics. 1992. 1-25. Print.

Kapteyn-Murnane Laboratories L.L.C. *Frequency Resolved Optical Gating (FROG) Hardware Manual*; *Version 2.10*. 30 Aug 2002. Print.

Kapteyn-Murnane Laboratories L.L.C. *Instruction Manual: Model TS Ti:sapphire laser kit*. 27 July 2000. 2-14. Print.

Miller, Jonah Maxwell. *Optimizing and Applying Graphene as a Saturable Absorber For Generating Ultrashort Pulses*. University of Colorado. 2011. iii, 7. PDF. http://www.thephysicsmill.com/blog/wp-content/uploads/jm_thesis_draft_3.pdf

NKT Photonics. *Supercontinuum Generation in Photonic Crystal Fibers*. July 2009. Web. http://www.thorlabs.com/images/TabImages/Supercontinuum%20-%20General%20Application%20Note%20-%20Thorlabs.pdf

Pedrotti, Frank L., and Leno S. Pedrotti. *Introduction to Optics; Second Edition*. New Jersey: Prentice Hall, Inc. 1993. 542, 551-552. Print.

Pe'er, Avi, and Shai Yefet. *A Review of Cavity Design for Kerr Lens Mode-Locked Solid-State Lasers*. Bar-Ilan University. 10 Dec 2013. 696-699. 710-712. Web.

Ranka, Jinendra K., Robert S. Windeler, and Andrew J. Stentz. *Visible Continuum Generation in Air-Silica Microstructure Optical Fibers with Anomalous Dispersion at 800 nm*. 13 Oct 1999. Print.

Taft, Greg. Kapteyn-Murnane Laboratories Inc. Technical Sales.

ThorLabs.com. *Highly Nonlinear PM PCF for 800nm Pump Lasers*. ThorLabs. 2015. Web. http://www.thorlabs.com/newgrouppage9.cfm?objectgroup_id=2044

Trebino, Rick. *Frequency-Resolved Optical Gating: The Measurement of Ultrashort Laser Pulses*. Boston: Kluwer Academic Publishers, 2000. 1-4, 367. Print and PowerPoint.